

Coupling enhancement and symmetrization of single-photon optomechanics in open quantum systems

Cheng Shang ^{*1}

¹*Department of Physics, The University of Tokyo, 5-1-5 Kashiwanoha, Kashiwa, Chiba 277-8574, Japan*
(Dated: February 13, 2023)

A challenging task of cavity optomechanics is to observe single-photon optomechanical effects. To explore an intrinsic nonlinear effect of single-photon cavity optomechanics, we need to strengthen the radiation-pressure (RP) interaction between a single photon and a finite number of phonons. In this work, introducing the two-laser driving and considering the second-order correction to the cavity resonance frequency beyond the RP interaction, we realize controllable enhancement of the single-photon optomechanical coupling in a prototypical Fabry-Pérot cavity. By adjusting the parameters of the two driving lasers and the cross-Kerr (CK) interaction so that the effective optomechanical coupling may become a real number, we theoretically propose effective symmetric optomechanical dynamics at the single-photon level, in which the forms of the quantum fluctuation dynamics satisfied by the photon and phonon are identical to each other. We study optimal reciprocal transport in symmetric optomechanics. By observing the critical behavior of the optimal transmission of the laser field, we identify the boundary point of the optomechanical strong coupling. We compare the scattering behavior of the laser field in the dissipative equilibrium and non-equilibrium symmetric optomechanics before and after the rotating-wave approximation (RWA). We also present a reliable experimental implementation of the present scheme. This work may pave the way to studying the single-photon optomechanical effects with current experimental platforms.

I. INTRODUCTION

Cavity optomechanics is a rapidly developing research field involving quantum optics and nanoscience [1–3]. Work in this field aims to study the radiation-pressure (RP) coupling between electromagnetic and mechanical degrees of freedom [4–6]. Recently, particular interest has focused on theoretically exploring single-photon optomechanical effects [7–9] since exploiting the intrinsic nonlinear RP interaction of the cavity optomechanics would open the doors to a much vaster realm of possibilities in the quantum regime. Many unusual phenomena appear in this regime, such as the appearance of phonon sidebands in the cavity emission spectrum [10], the photon blockade effect due to a weakly driving laser [11–14], and the generation of macroscopic quantum superposition [15, 16].

However, the single-photon optomechanical effects have not been observed yet under existing experimental techniques. It is because the single-photon optomechanical coupling is too weak to be distinguished from the environmental noise in the standard optomechanical systems [17]. In the field of cavity optomechanics, how to reinforce the coupling to reach the regime of strong single-photon coupling is still one of the non-trivial challenges.

So far, many schemes have been proposed for the enhancement of the single-photon optomechanical coupling. These schemes include the generation of collective density excitation of the Bose-Einstein condensate [18], the construction of an array of mechanical resonators [19], the usage of the squeezing cavity mode [20, 21], the exploitation of mechanical amplification [22], the application of delayed quantum feedback [23], and the utilization of the critical property of

the lower-branch polariton cavity coupling [24]. In addition, recently, an all-optical system based on a Fredkin-type interaction has been proposed to simulate the ultrastrong optomechanical coupling [25]. However, there are two common issues in these schemes [26]. One is how to guarantee that the system always works at the single-photon level. The other is how to ensure that we can observe the intrinsic nonlinear effects in an optomechanical system if it has other degrees of freedom.

Motivated to resolve these issues, in this paper, we focus on a novel strategy to enhance the nonlinear effects and reach the single-photon ultrastrong coupling regime without introducing any additional nonlinear sources in theory. First, we propose a method of realizing the controllable enhancement of single-photon optomechanical coupling in a prototypical Fabry-Pérot cavity. In contrast to the hybrid cavity optomechanics or optomechanical-like systems, we stress that our scheme is realized by considering only two points. One is the second-order correction to the cavity resonance frequency beyond the RP interaction, namely the cross-Kerr (CK) interaction [27, 28], which is an inherent nonlinear interaction accompanied by the optomechanical coupling [29–31]. The other is to make sure that the mechanical resonator and the optical cavity are driven by an appropriate high-power laser [32, 33] and a low-power one [34], respectively. Second, by adjusting the parameters of the two driving lasers and the CK interaction so that the effective optomechanical coupling may become a real number, we theoretically propose effective symmetric optomechanical dynamics at the single-photon level, in which the forms of the quantum fluctuation dynamics satisfied by the photon and phonon are identical to each other. Third, we control the coupling strength of single-photon optomechanical dynamics by laser driving and the CK interaction, achieving sequential transitions from weak coupling to ultrastrong coupling regime [35, 36]. By observing the critical behavior of the optimal transmission of the laser field, we

^{*}c-shang@iis.u-tokyo.ac.jp

identify the boundary point of the optomechanical strong coupling. In addition, we study the optimal reciprocal transport in symmetric optomechanical dynamics [37–39]. We compare the scattering behavior of the laser field when the decay rate of the cavity field matches the damping rate of the mechanical oscillator or not before and after the rotating-wave approximation (RWA). We also present a reliable experimental implementation of the present scheme through a quantum electrodynamics (QED) circuit of superconducting qubits.

The remainder of this paper is organized as follows in Sec. II, we introduce the physical model and derive the dynamic equations satisfied by the system. In Sec. III, we propose effective symmetric optomechanics at the single-photon level, and estimate the number of photons and phonons in this system. In Sec. IV, we study the transmission behavior of the laser field in this symmetric optomechanical system before and after the RWA. In Sec. V, we present an experimental implementation of the present scheme. In Sec. VI, we conclude and present a prospect.

II. COUPLING CONTROL OF OPTOMECHANICAL SYSTEMS

A. Derivation of controllable coupling model

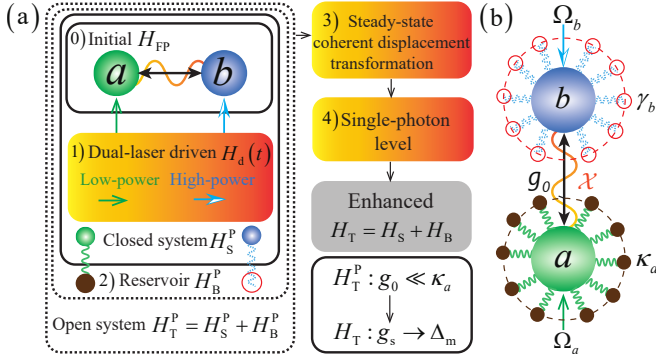


FIG. 1: (a) A flowchart for obtaining an enhanced Hamiltonian H_T . Initially, we consider a primitive (undriven) Fabry-Pérot cavity H_{FP} . The first step is to introduce two laser beams $H_d(t)$ to drive the initial system. Next, we extend the above closed system H_S^P to an open quantum system H_T^P by adding an environmental Hamiltonian H_B^P . Then, we perform a steady-state coherent displacement transformation on it. As the last step, we omit the CK interaction term to obtain an enhanced Hamiltonian H_T at the single-photon level. (b) Schematic illustration of a generalized optomechanical model H_T^P [left side of (a)], which is composed of a single-mode optical field a (lower side) and a mechanical mode b (upper side). The optical mode is coupled to the mechanical mode via both the RP interaction g_0 (\leftrightarrow) and the CK interaction χ (\sim). The optical mode is driven by a low-power laser Ω_a , while the mechanical mode is driven by a high-power laser Ω_b . In addition, the near-resonant coupling between the system modes and their corresponding reservoir modes is also considered in this open quantum system.

For the standard cavity optomechanical system, the single-photon optomechanical coupling g_0 is far less than the de-

cay rate of the optical cavity κ_a . We present in Fig. 1(a) the processes of making the prototypical optomechanical system achieve an ultrastrong coupling g_s by laser-driven control in an open system. Here by ultrastrong coupling, we mean the case in which the strengthened single-photon optomechanical coupling g_s is a considerable fraction of the detuning of the mechanical resonance frequency Δ_m [40]. The derivation of an enhanced model in an open quantum system involves four steps described below.

Initially, as the simplest optical resonator structure, we consider a generic Fabry-Pérot cavity consisting of a single-mode optical cavity field and a single-mode mechanical oscillator [see Fig. 1(b)]. Here we consider the lowest-order correction of interaction beyond the radiation-pressure (RP) term, namely the cross-Kerr (CK) interaction term [see Appendix A for details [41–44]]. This leads to the Hamiltonian of the generalized optomechanical model that reads

$$H_{FP} = \hbar\omega_c a^\dagger a + \hbar\omega_m b^\dagger b - \hbar g_0 a^\dagger a (b^\dagger + b) + \hbar\chi a^\dagger a b^\dagger b, \quad (1)$$

where a^\dagger (a) and b^\dagger (b) are the creation (annihilation) operators of the optical mode and the mechanical mode with the corresponding resonance frequencies ω_c and ω_m , respectively. The third term describes the RP coupling between the two modes, where g_0 is the vacuum optomechanical coupling strength in the unit of frequency. It quantifies the interaction between a single phonon and a single photon. The fourth term, on the other hand, denotes the CK interaction between the two modes with the coupling strength χ , which can be strengthened experimentally by utilizing the Josephson junctions [45] or the superconducting qubits [46]. In this work, we use an enhanced CK nonlinear dominant optomechanical interaction, which means that the CK nonlinearity in Eq. (1) is much greater than the RP nonlinearity [47–49]. Therefore we omit the third term in Eq. (1) and obtain an approximate Hamiltonian as $H_{FP}^{app} = \hbar\omega_c a^\dagger a + \hbar\omega_m b^\dagger b + \hbar\chi a^\dagger a b^\dagger b$. The photon number is a conserved quantity in it because of the commutation relation $[a^\dagger a, H_{FP}] = 0$.

The first step: in order to enhance the single-photon optomechanical coupling, we introduce dual-laser driving to the system described by the approximate Hamiltonian H_{FP}^{app} . The driving Hamiltonian is given by

$$H_d(t) = \hbar(\Omega_a^* a e^{i\omega_{L_a} t} + \Omega_b^* b e^{i\omega_{L_b} t}) + \text{H.c.}, \quad (2)$$

where the optical mode is driven by a weak monochromatic field with ω_{L_a} and Ω_a being the driving frequency and complex amplitude, respectively. The mechanical mode, on the other hand, is driven by a strong monochromatic field, where ω_{L_b} and Ω_b are the driving frequency and complex amplitude, respectively. The total Hamiltonian of the closed system is now given by $H_S^P(t) = H_{FP}^{app} + H_d(t)$. To make the Hamiltonian independent of time, we then move to the rotating frame of the frequency, which makes the Hamiltonian of the closed system as follows:

$$\begin{aligned} H_S^P &= +U(t) H_S^P(t) U^\dagger(t) - iU(t) \dot{U}^\dagger(t) \\ &= +\hbar\Delta_c a^\dagger a + \hbar\Delta_m b^\dagger b + \hbar\chi a^\dagger a b^\dagger b \\ &\quad + \hbar(\Omega_a^* a + \Omega_b^* b + \text{H.c.}), \end{aligned} \quad (3)$$

where we used the unitary transformation of the form $U(t) = \exp[i(\omega_{L_a} a^\dagger a + \omega_{L_b} b^\dagger b)t]$. The parameter $\Delta_c = \omega_c - \omega_{L_a}$ is the detuning of the resonant frequency ω_c of the optical cavity a from the driving frequency ω_{L_a} , while $\Delta_m = \omega_m - \omega_{L_b}$ is the detuning of ω_m of the mechanical oscillator b from the driving frequency ω_{L_b} . Note that we will adopt circuit quantum electrodynamics (circuit-QED) [50–52] to achieve (3) at the single-photon level, that is, to make the excitation number of the optical mode a approximately one, and hence the third term will be much smaller than the second because $\chi \approx 10^{-3} \Delta_m$. However, to realize the enhancement of radiation-pressure interaction by means of the nonlinear CK interaction, we retain the third term now. The second step: in order to extend the system to an open quantum one, we further add a system-reservoir interaction using a quantum operator approach [53]. The total Hamiltonian of this field-reservoir system is now written as $H_T^P = H_S^P + H_B^P$ with

$$H_B^P = + \sum_k \hbar \left[\omega_{ak} \Gamma_{ak}^\dagger \Gamma_{ak} + g_{ak} \left(a^\dagger \Gamma_{ak} + a \Gamma_{ak}^\dagger \right) \right] + \sum_k \hbar \left[\omega_{bk} \Gamma_{bk}^\dagger \Gamma_{bk} + g_{bk} \left(b^\dagger \Gamma_{bk} + b \Gamma_{bk}^\dagger \right) \right], \quad (4)$$

where Γ_{ak}^\dagger (Γ_{ak}) and Γ_{bk}^\dagger (Γ_{bk}) are, respectively, the creation (annihilation) operators of the reservoirs for the optical mode and the mechanical mode. The present reservoir consists of many harmonic oscillators with closely spaced frequencies ω_{ak} (ω_{bk}). The g_{ak} and g_{bk} terms represent the corresponding system-reservoir interactions.

The third step: to achieve steady-state coupling enhancement of a prototypical optomechanics in open quantum systems, we modulate the detuning of the resonant frequency of the optical cavity Δ_c by driving the mechanical oscillator b (the movable mirror) with appropriate high-power laser Ω_b , thereby enhancing the underlying single-photon optomechanical coupling; that is, when the mechanical oscillator is driven by a specific intense monochromatic laser Ω_b that satisfies $|\Omega_b| \gg |\Omega_a|$, the excitation number in the mechanical mode b is large, and then b contains a steady-state coherent part β_s . In other words, we employ the coherent-displacement transformation [54, 55] of the mechanical mode of the form $D(\beta) b D^\dagger(\beta) = b - \beta$ and $D(\beta) b^\dagger D^\dagger(\beta) = b^\dagger - \beta^*$, where the unitary displacement operator is given by $D_b(\beta) = \exp(\beta b^\dagger - \beta^* b)$ in the coherent-state representation. Since our purpose here is to obtain an optomechanical coupling enhancement at a steady state, in the following, we focus on the steady-state displacement solution β_s ; we assume that the timescale of the system approaching its steady state is much shorter than other evolution timescales. The specific form of β_s will be given by the dynamics equation later. The total Hamiltonian H_T^P after the transformation can be written as $H_T^{\text{tra}} = H_S + H_B$ with

$$H_S = \hbar \Delta_c^0 a^\dagger a + \hbar (\Delta_m + \chi a^\dagger a) b^\dagger b - \hbar \chi a^\dagger a (\beta_s b^\dagger + \beta_s^* b) + \hbar (\Omega_a^* a + \Omega_b^* b - \beta_s^* \Delta_m b + \text{H.c.}) + \hbar \Delta_m \beta_s^* \beta_s - \hbar \Omega_b^* \beta_s - \hbar \Omega_b \beta_s^*, \quad (5)$$

$$H_B = H_B^P - \hbar \sum_k g_{bk} \left(\beta_s^* \Gamma_{bk} + \beta_s \Gamma_{bk}^\dagger \right), \quad (6)$$

where $\Delta_c^0 = \Delta_c + \chi \beta_s^* \beta_s$ is the normalized optical cavity detuning including the frequency shift caused by the high-power laser driving.

The fourth step: since β_s is controlled by the mechanical laser driving, we can enhance the coupling in the form $\chi \beta_s$. After the coherent-displacement transformation at the steady state, the RP coupling reads $\hbar a^\dagger a (g_s b^\dagger + g_s^* b)$, where $g_s = \chi \beta_s$. We then omit the CK interaction term in Eq. (5) [56], obtaining the final enhanced Hamiltonian H_T (after shifting the origin of the energy) as follows

$$H_T = + \hbar \Delta_c^0 a^\dagger a + \hbar \Delta_m b^\dagger b - \hbar a^\dagger a (g_s b^\dagger + g_s^* b) + \hbar (\Omega_a^* a + \Omega_b^* b - \beta_s^* \Delta_m b + \text{H.c.}) + H_B. \quad (7)$$

We thus manage to enhance single-photon optomechanical coupling g_0 in Eq. (1) at the level of a single photon and a single phonon to g_s in Eq. (7) at the level of a single photon and finite phonon.

B. Nonlinear quantum Langevin equations

To introduce quantum damping and noise in Eq. (7) and to give the specific form of β_s , we now describe the coupling between the system and the reservoir in terms of input-output formalism [57]. This formalism provides us with equations of motion for the amplitude of the optical cavity field a and analogously for the mechanical amplitude b . Substituting the final enhanced Hamiltonian H_T into the Heisenberg equation and taking the dissipation terms with κ_a and γ_b as well as the corresponding noise terms with a_{in} and b_{in} into account, we find a set of closed integro-differential equations for the operators of the optical mode and mechanical mode as follows

$$\dot{a} = \frac{1}{i\hbar} [a, H_T] = - \left[i \Delta_c^0 + \frac{\kappa_a}{2} - i (g_s b^\dagger + g_s^* b) \right] a - i \Omega_a + \sqrt{\kappa_a} a_{\text{in}}, \quad (8)$$

$$\dot{b} = \frac{1}{i\hbar} [b, H_T] = - \left(i \Delta_m + \frac{\gamma_b}{2} \right) b + i g_s a^\dagger a + \sqrt{\gamma_b} b_{\text{in}} + \dot{\beta}_s, \quad (9)$$

where κ_a is the decay rate of the optical cavity field, γ_b is the mechanical damping rate.

The time derivative of the steady-state displacement amplitude $\dot{\beta}_s$ is equal to zero. See Appendix B for a detailed derivation of the Heisenberg-Langevin equation [58, 59]. From the results in Appendix B, we can see that the condition for the Heisenberg-Langevin equation to remain unchanged after the coherent displacement transformation is $\dot{\beta}(t) + (i \Delta_m + 0.5 \gamma_b) \beta(t) - i \Omega_b = 0$. The solution gives the transient displacement amplitude $\beta(t)$ depending on the mechanical laser drive Ω_b in the form $\beta(t) = \Omega_b / (\Delta_m - i 0.5 \gamma_b) + C(t_0) \exp[-(i \Delta_m + 0.5 \gamma_b) t]$. In the long-time limit, the second term on the right-hand side converges to zero, and we find the steady-state coherent displacement amplitude $\beta_s = \Omega_b / (\Delta_m - i 0.5 \gamma_b)$. An alternative viewpoint, namely the Gorini-Kossakowski-Sudarshan-Lindblad (GKSL) master equation [60, 61] on the evaluation of the steady-state displacement amplitude β_s can be found in Appendix C [56].

Within the Born-Markov approximation [62], the incoming vacuum noise a_{in} of the optical cavity field in Eq. (8) and the thermal noise b_{in} of the mechanical oscillator in Eq. (9) are fully characterized by the following correlation functions:

$$\begin{aligned} \langle a_{\text{in}} \rangle &= 0, \quad \langle a_{\text{in}}^\dagger(t) a_{\text{in}}(t') \rangle = 0, \\ \langle a_{\text{in}}(t) a_{\text{in}}^\dagger(t') \rangle &= \delta(t - t'), \end{aligned} \quad (10)$$

$$\begin{aligned} \langle b_{\text{in}} \rangle &= 0, \quad \langle b_{\text{in}}^\dagger(t) b_{\text{in}}(t') \rangle = \bar{n}_m \delta(t - t'), \\ \langle b_{\text{in}}(t) b_{\text{in}}^\dagger(t') \rangle &= (\bar{n}_m + 1) \delta(t - t'). \end{aligned} \quad (11)$$

Here, \bar{n}_m is the mean thermal excitation number of the mechanical reservoir under thermal equilibrium. Equations (8) and (9) have the form of the nonlinear QLEs since both the light amplitude and the mechanical motion are driven by noise terms that comprise the vacuum noise and the thermal noise entering the system. Together with Eqs. (10) and (11), the nonlinear QLEs describe the evolution of the optical cavity field and the mechanical oscillator, including dissipations (κ_a, γ_b) and incoming noises ($a_{\text{in}}, b_{\text{in}}$).

In order to find the standard form of the nonlinear QLEs, we consider the particular case in which the steady-state displacement amplitude β_s satisfies the following condition:

$$\beta_s = \beta_s^* = |\beta_s| = \beta_s^R > 0. \quad (12)$$

In other words, the steady-state displacement amplitude β_s is real and positive, which is specifically denoted by β_s^R . By assuming the laser amplitude $\Omega_b = i\varepsilon_b \exp(i\varphi_b)$, where ε_b denotes the laser power and φ_b denotes the phase of the laser field coupling to the mechanical mode, we obtain the steady-state solution satisfying Eq. (12) as

$$\beta_s^R = -\frac{2\varepsilon_b \cos(\varphi_b)}{\gamma_b} \geq 0, \quad \tan(\varphi_b) = \frac{2\Delta_m}{\gamma_b} \geq 0 \quad (13)$$

with $\varphi_b \in [\pi, 1.5\pi)$. Meeting the above conditions, we arrive at the standard nonlinear QLEs as follows:

$$\dot{a} = -\left(i\Delta_c^0 + \frac{\kappa_a}{2}\right)a + ig(b^\dagger + b)a + \sqrt{\kappa_a}a_{\text{in}} - i\Omega_a, \quad (14)$$

$$\dot{b} = -\left(i\Delta_m + \frac{\gamma_b}{2}\right)b + ig a^\dagger a + \sqrt{\gamma_b}b_{\text{in}}, \quad (15)$$

where $g_s = g_s^* = g = \chi\beta_s^R$ is the controllable optomechanical coupling strength at the single-photon level.

III. SYMMETRICAL OPTOMECHANICAL DYNAMICS AT SINGLE-PHOTON LEVEL

A. Real optomechanical coupling

The nonlinear QLEs. (14) and (15) are inherently nonlinear as they contain products of photon (optical cavity field) and phonon (mechanical oscillator amplitude) operators, ab and ab^\dagger , and a quadratic term in photon operators, $a^\dagger a$. Taking the standard mean-field method in order to solve Eqs. (14) and

(15), we start by splitting the photon and phonon operators into the classical mean values and quantum fluctuation operators, i.e., $a = \alpha + \delta a$ with $a^\dagger = \alpha^* + \delta a^\dagger$ and $b = \eta + \delta b$ with $b^\dagger = \eta^* + \delta b^\dagger$. Adopting the above approach, the solution of the complex mean values for the classical steady state satisfies

$$\dot{\alpha} = -\left(i\Delta_c^0 + \frac{\kappa_a}{2}\right)\alpha + ig(\eta^* + \eta)\alpha - i\Omega_a, \quad (16)$$

$$\dot{\eta} = -\left(i\Delta_m + \frac{\gamma_b}{2}\right)\eta + ig|\alpha|^2. \quad (17)$$

By solving Eqs. (16) and (17), we obtain the solution of the complex mean values α and η for the classical steady state as follows:

$$\begin{aligned} \alpha &= \frac{-i\Omega_a \left[\left(\frac{\gamma_b}{2}\right)^2 + (\Delta_m)^2 \right]}{\left(i\Delta_c^0 + \frac{\kappa_a}{2}\right) \left[\left(\frac{\gamma_b}{2}\right)^2 + (\Delta_m)^2 \right] - 2ig^2\Delta_m|\alpha|^2}, \\ \eta &= \frac{ig|\alpha|^2}{i\Delta_m + \frac{\gamma_b}{2}}, \end{aligned} \quad (18)$$

which depend on the average photon number $|\alpha|^2 = N_{\text{cav}} \approx 1$ circulating inside the optical cavity.

The quantum fluctuations δa and δb satisfy the following nonlinear equations of motion:

$$\begin{aligned} \delta \dot{a} &= -\left(i\Delta_c' + \frac{\kappa_a}{2}\right)\delta a + ig\alpha(\delta b^\dagger + \delta b) \\ &\quad + ig\delta a(\delta b^\dagger + \delta b) + \sqrt{\kappa_a}\delta a_{\text{in}}, \end{aligned} \quad (19)$$

$$\begin{aligned} \delta \dot{b} &= -\left(i\Delta_m + \frac{\gamma_b}{2}\right)\delta b + ig(\alpha\delta a^\dagger + \alpha^*\delta a) \\ &\quad + ig\delta a^\dagger\delta a + \sqrt{\gamma_b}\delta b_{\text{in}}, \end{aligned} \quad (20)$$

where we set renormalization of the detuning frequency of the optical cavity field as $\Delta_c' = \Delta_c^0 - g(\eta + \eta^*)$. To further solve Eqs. (19) and (20), we introduce a linearized mean-field approximation [63, 64] by dropping the contribution of terms of second orders in quantum fluctuations and keeping only the linear terms in Eqs. (19) and (20). We thereby obtain the linearized QLEs as follows:

$$\delta \dot{a} = -\left(i\Delta_c' + \frac{\kappa_a}{2}\right)\delta a + ig\alpha(\delta b^\dagger + \delta b) + \sqrt{\kappa_a}\delta a_{\text{in}}, \quad (21)$$

$$\delta \dot{b} = -\left(i\Delta_m + \frac{\gamma_b}{2}\right)\delta b + ig(\alpha\delta a^\dagger + \alpha^*\delta a) + \sqrt{\gamma_b}\delta b_{\text{in}}, \quad (22)$$

which are easy to solve analytically in the frequency domain after Fourier transformation. Furthermore, by observing the form of Eqs. (21) and (22), we find that Eq. (21), which describes the dynamical evolution of the photon fluctuation operator, and Eq. (22), which depicts the dynamical behavior of the phonon fluctuation operator, are completely symmetrized when we meet the following two scenarios simultaneously in this open quantum system.

The first scenario is to set the average value α of the photons in the classical steady state to a real number α_R . With this restriction, we can determine the real mean value of the classical steady state of the photons α_R and η_{α_R} (the value of

η for a fixed value α_R) from Eqs. (16) and (17) as follows:

$$\varepsilon_a \cos(\varphi_a) - \frac{\kappa_a}{2} \alpha_R = 0, \quad (23)$$

$$ig(\alpha_R)^2 - \left(i\Delta_m + \frac{\gamma_b}{2}\right) \eta_{\alpha_R} = 0, \quad (24)$$

$$\varepsilon_a \sin(\varphi_a) - \alpha_R \Delta_c'' = 0, \quad (25)$$

where we set the laser amplitude Ω_a to $i\varepsilon_a \exp(i\varphi_a)$ with ε_a denoting the laser power and φ_a the phase of the laser field coupling to the optical mode. We also defined $\Delta_c'' = \Delta_c^0 - g(\eta_{\alpha_R} + \eta_{\alpha_R}^*)$ as a modified detuning frequency of the optical cavity field. We can transform Eqs. (23)-(25) as follows:

$$\alpha_R = \frac{2\varepsilon_a \cos(\varphi_a)}{\kappa_a}, \quad \eta_{\alpha_R} = \frac{2ig(\alpha_R)^2}{2i\Delta_m + \gamma_b}, \quad (26)$$

$$\tan(\varphi_a) = \frac{2\Delta_c''}{\kappa_a} = \frac{2}{\kappa_a} [\Delta_c^0 - g(\eta_{\alpha_R} + \eta_{\alpha_R}^*)]. \quad (27)$$

Substituting Eq. (26) into Eq. (27), we obtain a nonlinear equation for φ_a in the form

$$\tan(\varphi_a) = \frac{2}{\kappa_a} \left\{ \Delta_c^0 - \frac{8\Delta_m}{4(\Delta_m)^2 + (\gamma_b)^2} \left[\frac{2g\varepsilon_a \cos(\varphi_a)}{\kappa_a} \right]^2 \right\}. \quad (28)$$

Note that since $\alpha_R > 0$, we find the solution of Eq. (28) in the range: $\varphi_a \in [0, 0.5\pi) \cup (1.5\pi, 2\pi]$. If we consider α as a complex mean value satisfying the classical steady-state solution (18), the phase of the complex number α destroys the symmetrical form of dynamics, resulting in non-reciprocal transmission [65].

Now, substituting the expressions (26) into Eqs. (21) and (22), we can reduce them to the following forms:

$$\delta\dot{a} = -\left(i\Delta_c'' + \frac{\kappa_a}{2}\right) \delta a + iG_R (\delta b^\dagger + \delta b) + \sqrt{\kappa_a} \delta a_{\text{in}}, \quad (29)$$

$$\delta\dot{b} = -\left(i\Delta_m + \frac{\gamma_b}{2}\right) \delta b + iG_R (\delta a^\dagger + \delta a) + \sqrt{\gamma_b} \delta b_{\text{in}}, \quad (30)$$

where $G_R = g\alpha_R$ is an effective optomechanical coupling in the linearized regime. It is enhanced compared to g by the real amplitude α_R of the photon field.

Equations (29) and (30) show the formal equivalence of the quantum fluctuation dynamics of photons and phonons. The corresponding effective Hamiltonian of the system under the Heisenberg picture (time-dependent operator) is given by $H_{\text{eff}} = \hbar\Delta_c'' a^\dagger a + \hbar\Delta_m b^\dagger b - \hbar G_R (a^\dagger + a)(b^\dagger + b)$. Hereafter, we refer to H_{eff} as the effective Hamiltonian of the symmetric optomechanical system, in which the interaction part describes a general linear interaction between two boson modes in the field of quantum optics. Besides, we know that the Hamiltonian of the Jaynes-Cummings model describing the atom-field interaction has a similar interaction form $\hbar g(a^\dagger + a)(\sigma_+ + \sigma_-)$, where the operator σ_+ takes an atom in the lower state into the upper state whereas σ_- has the opposite effect. Therefore, we say that the effective symmetric Hamiltonian H_{eff} describes the most general linear interaction between light and matter. The results obtained in physics are

universal for studying the interaction between light and matter.

The other scenario to find the complete equivalence of the quantum fluctuation dynamics of photon and phonon is to set the corresponding parameters in Eqs. (29) and (30) equal to each other. To be specific, we equalize the modified detuning frequency Δ_c'' of the optical cavity field to the detuning of the mechanical resonance frequency Δ_m by adjusting the two driving lasers Ω_a and Ω_b . We also equalize the decay κ_a of the optical cavity field to the damping γ_b of the mechanical oscillator by modulating the corresponding system-reservoir interaction g_{ak} and g_{bk} . To implement this scenario, we carefully analyze and compare representative works in the theoretical proposal and experimental results concerning the optomechanical systems with the CK interaction; see Table I. We see that the circuit quantum electrodynamics (circuit-QED) systems may be a promising platform for realizing this scenario, in which the parameter conditions $\Delta_c'' = \Delta_m$ and $\kappa_a = \gamma_b$ can be satisfied.

If the above two scenarios are satisfied, the quantum fluctuation dynamics of photons and phonons are completely symmetrized. Equations (29) and (30) now read

$$\delta\dot{a} = -\left(i\Delta + \frac{\xi}{2}\right) \delta a + iG_R (\delta b^\dagger + \delta b) + \sqrt{\xi} \delta a_{\text{in}}, \quad (31)$$

$$\delta\dot{b} = -\left(i\Delta + \frac{\xi}{2}\right) \delta b + iG_R (\delta a^\dagger + \delta a) + \sqrt{\xi} \delta b_{\text{in}}, \quad (32)$$

where $\Delta = \Delta_c'' = \Delta_m$ and $\xi = \kappa_a = \gamma_b$. Equations (31) and (32) describe the quantum fluctuation dynamics of the completely symmetric optomechanics in open quantum systems. The symmetrization of the quantum fluctuation dynamics of photons and phonons reveals a more profound connection under quantum mechanics; namely, both are bosons.

B. Implementation of optomechanical strong coupling at the single-photon level

As shown in Fig. 2, in the symmetric optomechanical Eqs. (31) and (32), we adopt the form of the dual laser driving in order to achieve an optomechanical strong coupling at the single-photon level. On the one hand, a lower-power monochromatic laser Ω_a drives the optical cavity a to excite a small number of photons \bar{N}_a in the optical cavity. On the other hand, a high-power monochromatic laser Ω_b drives the mechanical oscillator b so that steady-state displacement amplitude β_s may be large enough to achieve strong optomechanical coupling. Here, the single-photon optomechanical coupling refers to the interaction between a photon and a finite number of phonons. To achieve our goal, we need to do two things. One is to evaluate the power of the laser field driving the optical cavity to ensure that the number of photons acting on the system is approximately one. The other is to estimate the relationship between the laser power of the driving mechanical oscillator and the steady-state displacement amplitude in order to achieve strong optomechanical coupling.

TABLE I: Representative works in theoretical proposals and experimental results for various optomechanical systems with the CK interaction. Typical parameters of the standard cavity optomechanical system satisfy $\Delta_c'' = \Delta_c$. The blue part shows the maximum parameter values achieved by the system (5)-(6) simulated by the QED circuit after laser adjustment.

References	Type (Hz)	$\Delta_c''/2\pi$	$\Delta_m/2\pi$	$\kappa_a/2\pi$	$\gamma_b/2\pi$	$\chi/2\pi$
[49–52, 56]	Circuit-QED	5.2×10^9	5.2×10^9	3.3×10^7	3.3×10^7	2.5×10^6
[66, 67]	Cavity-QED	4.8×10^9	7.2×10^7	4.2×10^7	2.6×10^6	$10^4 \sim 10^5$
[68, 69]	Cavity-optomechanics	1.1×10^7	7.8×10^7	7.1×10^6	3.4×10^3	≈ 0
[70, 71]	Quadratic-optomechanics	2.8×10^{14}	1.3×10^6	5.9×10^5	1.2×10^{-1}	3.95×10^{-2}

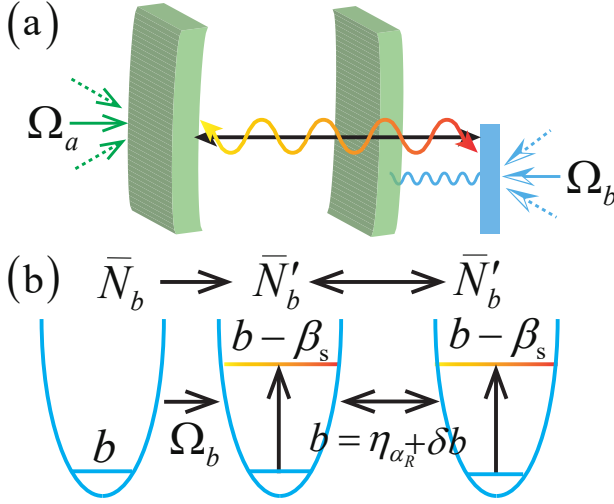


FIG. 2: (a) Schematic diagram of a symmetric optomechanical system with dual laser drives. (b) The number of excited phonons in the system after the coherent displacement transformation at the steady state and the standard mean-field operation.

First, we evaluate the relationship between the number of photons in the system and the low-power driving laser. We know from Eq. (26) that the average photon number acting on the symmetrical optomechanical system is given by

$$\bar{N}_a = \alpha_R^2 = 2 \left(\frac{\varepsilon_a}{\kappa_a} \right)^2 [\cos(2\varphi_a) + 1], \quad (33)$$

in which ε_a is related to the driving laser power P_a by $\varepsilon_a = |\Omega_a| = \sqrt{2P_a\kappa_a/\hbar\omega_{L_a}}$. Equation (33) is therefore rewritten as

$$0 \leq \bar{N}_a = \frac{4P_a [\cos(2\varphi_a) + 1]}{\hbar\omega_{L_a}\kappa_a} \leq \frac{8P_a}{\hbar\omega_{L_a}\kappa_a}. \quad (34)$$

For simplicity, we assume that the driving laser frequency ω_{L_a} of the optical cavity field is resonant with the modified detuning frequency of the optical cavity field Δ_c'' . In Fig. 3(a), we show that the average photon number \bar{N}_a in the optical cavity varies with the power P_a and the phase φ_a of the driving laser Ω_a . We find from Fig. 3(a) that we can make the number of photons acting in the optical cavity be unity by adjusting the phase φ_a from 0 to 0.5π and tuning the driving laser power P_a from 8.93×10^{-2} fW to infinity accordingly.

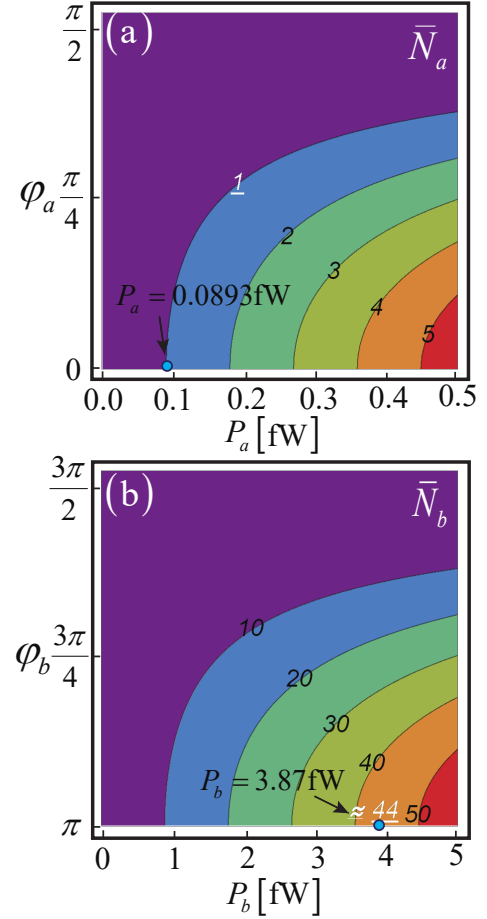


FIG. 3: (a) Average photon number \bar{N}_a in the optical cavity varies with the laser power $P_a \in [0, 0.5\text{fW}]$ and the phase $\varphi_a \in [0, 0.5\pi]$ of the optical driving laser field Ω_a . (b) The average number of thermally excited phonons \bar{N}_b varies with the laser power $P_b \in [0, 5\text{fW}]$ and the phase $\varphi_b \in [\pi, 1.5\pi]$ of the mechanical driving laser field Ω_b . Both (a) and (b) use the data of the circuit-QED in Table I: $\Delta_m = \omega_{L_a} = \omega_{L_b} = 1.04\pi \times 10^{10}\text{Hz}$, $\kappa_a = \gamma_b = 6.6\pi \times 10^7\text{Hz}$, $\chi = 5\pi \times 10^6\text{Hz}$, and $\hbar = 1.05 \times 10^{-34}\text{J} \cdot \text{s}$.

It is worthwhile to note that \bar{N}_a is proportional to P_a , except where $\varphi_a = 0.5\pi + n\pi$ with $n \in \mathbb{Z}$; for example, when $\varphi_a = 0$, $\bar{N}_a = (8/\hbar\omega_{L_a}\kappa_a) P_a$.

Under the premise that \bar{N}_a is unity, we now find how strong the laser power P_b we need to achieve an optomechanical strong coupling G_R . More specifically, it has been

TABLE II: Regimes of optomechanical interaction [76] and corresponding β_s^R and P_b ($\varphi_b = \pi$).

G_R	g_0	$0.5\kappa_a$	$0.1\Delta_m$	Δ_m	$> \Delta_m$	β_s^R	P_b	\bar{N}_b
Weak	•	◦				[0, 6.6)	[0, 3.87fW)	(0, 44)
Strong		•	◦			[6.6, 208)	[3.87fW, 3.85pW)	(44, 4.326×10^4)
Ultrastrong			•	•		[208, 2080]	[3.85pW, 0.385nW]	(4.326×10^4 , 4.326×10^6)
Deep strong					*	> 2080	$> 0.385\text{nW}$	$> 4.326 \times 10^6$

found experimentally that the optomechanical coupling has four regimes, namely weak [72], strong [73], ultrastrong [74], and deep strong [75]. We compute the range of P_b to achieve each of the four regions.

Note that the effective optomechanical coupling has the form $G_R = g\alpha_R$ with $g = \chi\beta_s^R$. Under the single-photon level $\alpha_R = \sqrt{\bar{N}_a} = 1$, G_R can be written as $G_R = g = \chi\beta_s^R$. We know from Eq. (13) that β_s^R is proportional to the laser power by $\varepsilon_b = |\Omega_b| = \sqrt{2P_b\gamma_b/\hbar\omega_{L_b}}$. The expression (13) is therefore written as

$$\beta_s^R = -\frac{2\varepsilon_b \cos(\varphi_b)}{\gamma_b} = -\frac{2 \cos(\varphi_b)}{\gamma_b} \sqrt{\frac{2P_b\gamma_b}{\hbar\omega_{L_b}}} \quad (35)$$

with $\varphi_b \in [\pi, 1.5\pi)$. Similarly, we assume that the driving laser frequency ω_{L_b} of the mechanical mode is resonant with the detuning of mechanical resonance frequency Δ_m . Let us use the data of the circuit-QED in Table I: $\gamma_b = 6.6\pi \times 10^7 \text{Hz}$, $\omega_{L_b} = \Delta_m = 1.04\pi \times 10^{10} \text{Hz}$, $\chi = 5\pi \times 10^6 \text{Hz}$, and $\hbar = 1.05 \times 10^{-34} \text{J}\cdot\text{s}$. As shown in Table II, the necessary laser power P_b to ensure strong coupling and ultrastrong coupling are more than 3.87fW and 3.85pW, which is corresponding to $\beta_s^R = 6.6$ and $\beta_s^R = 208$, respectively.

Finally, let us find the number of phonons \bar{N}_b for each regime of P_b . From Eqs. (26) and (35) we know that the average phonon number working on the symmetric optomechanics is given by

$$\bar{N}_b = |\beta_s^R|^2 + |\eta_{\alpha_R}|^2 = |\beta_s^R|^2 + \frac{(G_R)^2}{\left(\frac{\gamma_b}{2}\right)^2 + (\Delta_m)^2}. \quad (36)$$

From Table II and Eq. (36), we find the number of phonons in the four regimes: in the weak coupling regime $\bar{N}_b \in (0, 44)$; in the strong coupling regime $\bar{N}_b \in (44, 4.326 \times 10^4)$; in the ultrastrong coupling regime $\bar{N}_b \in (4.326 \times 10^4, 4.326 \times 10^6)$; in the deep coupling regime \bar{N}_b more than 4.326×10^6 . It means that we achieve a strong coupling or even an ultrastrong coupling through the interaction between a single photon and a finite number of thermally excited phonons.

Substituting the expressions for G_R and β_s^R into Eq. (36), we obtain the relationship among the average number of thermally excited phonons \bar{N}_b , the driving laser power P_b and phase φ_b as follows:

$$\bar{N}_b = \frac{8P_b[\cos(\varphi_b)]^2}{\hbar\omega_{L_b}\gamma_b} \left[1 + \frac{\chi^2}{\left(\frac{\gamma_b}{2}\right)^2 + (\Delta_m)^2} \right] \quad (37)$$

with $\varphi_b \in [\pi, 1.5\pi)$. Figure 3(b) shows \bar{N}_b as a function of P_b and φ_b . We find that the lowest laser power entering the strong coupling is 3.87fW when $\varphi_b = \pi$, which is consistent with Table II.

To summarize, we can achieve strongly coupled optomechanical devices at the single-photon level in the circuit-QED with driving laser power as little as $P_a = 8.93 \times 10^{-2} \text{fW}$ and $P_b = 3.87 \text{fW}$ for $\varphi_a = \pi$ and $\varphi_b = \pi$, which is consistent with the assumption that a high-power laser drives the mechanical oscillator and a low-power laser drives the optical cavity, $P_b \gg P_a$; see Fig. 2(b).

IV. INPUT-OUTPUT THEORY

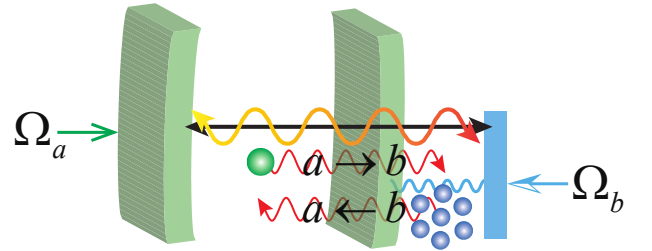


FIG. 4: Schematic diagram of a symmetric optomechanical system with dual laser drives at the single-photon level. The wavy line with $a \rightarrow b$ represents the transmission process of the photon signal from the optical cavity field to the mechanical oscillator, while the one with $b \rightarrow a$ describes the opposite process of the phonon signal.

In the preceding section, we obtain the Heisenberg-Langevin equation for a symmetric optomechanical system with a controllable coupling at the single-photon level. In this section, considering the input laser field shown in Fig. 4, we further derive the input-output formula of the incident laser field and study its scattering characteristics in the open quantum system. First, we numerically verify the conditions under which the rotating-wave approximation (RWA) holds in this system. Secondly, we give the conditions of the optimal reciprocal transmission of the incoming laser field in the system. We then compare the scattering behavior of the incident laser field in the dissipative balanced and unbalanced symmetric optomechanics before and after the RWA.

A. Applicability Conditions for Numerical Evaluation under RWA

In this part, we give the scattering matrix theory and evaluate the applicability of RWA by numerical calculation.

In the case without RWA, for convenience, we concisely express the linearized QLEs. (29)-(30) as

$$\dot{V} = -KV + \mu V_{\text{in}}, \quad (38)$$

where the component of each matrix is as follows: the quantum fluctuation operator is written as $V = (\delta a, \delta b, \delta a^\dagger, \delta b^\dagger)^T$; the noise field operator is denoted by $V_{\text{in}} = (\delta a_{\text{in}}, \delta b_{\text{in}}, \delta a_{\text{in}}^\dagger, \delta b_{\text{in}}^\dagger)^T$; the damping operators read $\mu = \text{diag}(\sqrt{\kappa_a}, \sqrt{\gamma_b}, \sqrt{\kappa_a}, \sqrt{\gamma_b})$; the coefficient matrix K in terms of system parameters takes the form

$$K = \begin{bmatrix} i\Delta_c'' + \frac{\kappa_a}{2} & -iG_R & 0 & -iG_R \\ -iG_R & i\Delta_m + \frac{\gamma_b}{2} & -iG_R & 0 \\ 0 & iG_R & -i\Delta_c'' + \frac{\kappa_a}{2} & iG_R \\ iG_R & 0 & iG_R & -i\Delta_m + \frac{\gamma_b}{2} \end{bmatrix}. \quad (39)$$

The system is stable only if the real parts of all the eigenvalues of the matrix K are positive. The eigenvalue equation $\det[K - \lambda I_4] = 0$, where I_4 denotes the four-dimensional identity matrix, can be reduced to the fourth-order equation $C_0\lambda^4 + C_1\lambda^3 + C_2\lambda^2 + C_3\lambda + C_4 = 0$. The stability conditions can be given by using the Routh-Hurwitz criterion as follows: $C_1 > 0, C_1C_2 - C_0C_3 > 0, (C_1C_2 - C_0C_3)C_3 - C_1^2C_4 > 0, C_4 > 0$ [77]. In the case without RWA, the following numerical calculations in this section ensure that the stability conditions are satisfied for the used parameters.

By introducing the Fourier transform for an operator $\Lambda(t)$ as

$$\Lambda(\omega) = \mathcal{F}[\Lambda(t)] = \frac{1}{\sqrt{2\pi}} \int_{-\infty}^{+\infty} \Lambda(t) e^{i\omega t} dt \quad (40)$$

and using its derivative property $\mathcal{F}[\dot{\Lambda}(t)] = -i\omega \mathcal{F}[\Lambda(t)]$, we find the solution to the linearized QLEs. (29)-(30) in the frequency domain in form

$$V(\omega) = [K - i\omega I_4]^{-1} \mu V_{\text{in}}(\omega), \quad (41)$$

Under boundary conditions, the relation among the input, internal, and output fields can be given by the input-output theory [78]. Substituting Eq. (41) into the input-output relation $V_{\text{out}}(\omega) + V_{\text{in}}(\omega) = \mu V(\omega)$, we obtain

$$V_{\text{out}}(\omega) = O(\omega) V_{\text{in}}(\omega), \quad (42)$$

in which the output field matrix $V_{\text{out}}(\omega)$ is the Fourier transform of $V_{\text{out}} = (\delta a_{\text{out}}, \delta b_{\text{out}}, \delta a_{\text{out}}^\dagger, \delta b_{\text{out}}^\dagger)^T$. The scattering matrix for the symmetric optomechanical system can be written as

$$O(\omega) = \mu^T [K - i\omega I_4]^{-1} \mu - I_4. \quad (43)$$

The spectrum of the output field is defined by

$$S_{\text{out}}(\omega) = \int d\omega' \langle V_{\text{out}}^\dagger(\omega') V_{\text{out}}(\omega) \rangle. \quad (44)$$

By substituting Eq. (42) into Eq. (44), we have

$$S_{\text{out}}(\omega) = P(\omega) S_{\text{in}}(\omega) + \Theta_{\text{vac}}(\omega), \quad (45)$$

where the term $P(\omega)$ denotes the scattering probability that corresponds to the contribution arising from the input laser field. The term $\Theta_{\text{vac}}(\omega)$ is a contribution of the input vacuum field to the output spectrum (see Ref. [79] for the explicit definition of the term), which is an effect of the anti-RWA terms [80]. Let us modify the results of Ref. [81]. The modified scattering probability has broad applicability, which is not only applicable to weak coupling but also suitable to strong coupling and even ultrastrong coupling [see Appendix D for details]. The functions $P(\omega)$ and $\Theta_{\text{vac}}(\omega)$ have the form

$$a \rightarrow b : P_a^b(\omega) = |O_a^b(\omega)|^2; \\ \Theta_{\text{vac}}^a(\omega) = |O_a^{\dagger}(\omega)|^2 + |O_a^b(\omega)|^2, \quad (46)$$

$$a \leftarrow b : P_b^a(\omega) = |O_b^a(\omega)|^2; \\ \Theta_{\text{vac}}^b(\omega) = |O_b^{\dagger}(\omega)|^2 + |O_b^a(\omega)|^2, \quad (47)$$

where $a \rightarrow b$ represents the transmission of the laser signal from the optical mode a to the mechanical mode b , while $a \leftarrow b$ denotes effects in the reverse process, and $O_a^b(\omega)$ represents the corresponding element at the first δa row and the second δb column of the scattering matrix $O(\omega)$ given in Eq. (43).

To calculate the scattering behavior of the incoming laser field in the symmetric optomechanics, we use the scattering matrix theory. For simplicity, taking the parameter values for the QED circuit in Table I, we have $\Delta_c'' = \Delta_m \approx 158\kappa_a = 158\gamma_b$, which satisfies the red detuned regime $\Delta_c'' = \Delta_m$ and sideband resolved regime $\text{Max}(\kappa_a, \gamma_b) \ll \Delta_m$ [82, 83], and thus we can apply the RWA to omit the anti-RWA terms $\delta a \delta b$ and $\delta a^\dagger \delta b^\dagger$, since they are strongly non-resonant; applying these terms to a state changes the total energy by an amount much larger than the coupling. Later, we verify numerically the rationality of the RWA applied here.

We now move to the RWA case. Keeping only the resonant terms $\delta a \delta b^\dagger$ and $\delta a^\dagger \delta b$ of the linearized QLEs. (29)-(30), we have

$$\dot{v} = -Mv + Lv_{\text{in}}, \quad (48)$$

where the quantum fluctuation vector is written as $v = (\delta a, \delta b)^T$. The noise operator is written in a matrix form $v_{\text{in}} = (\delta a_{\text{in}}, \delta b_{\text{in}})^T$. The damping operators in a matrix form read $L = \text{diag}(\sqrt{\kappa_a}, \sqrt{\gamma_b})$. The coefficient matrix M in terms of system parameters takes the form

$$M = \begin{bmatrix} i\Delta_c'' + \frac{\kappa_a}{2} & -iG_R \\ -iG_R & i\Delta_m + \frac{\gamma_b}{2} \end{bmatrix}, \quad (49)$$

The stability conditions for the system demand that the real parts of all the eigenvalues of the coefficient matrix M are

positive, which can be given by using the Routh-Hurwitz criterion. Using the parameter values for the QED circuit in Table I, we have $\Delta_c'' = \Delta_m = \Delta$ and $\kappa_a = \gamma_b = \xi$. Solving the eigenvalue equation $\det[M - \varepsilon I_2] = 0$, where I_2 denotes the two-dimensional identity matrix, we obtain two eigenvalues $\varepsilon_1 = i(\Delta - G_R) + \xi/2$ and $\varepsilon_2 = i(\Delta + G_R) + \xi/2$. We find that $\text{Re}[\varepsilon_1] = \text{Re}[\varepsilon_2] = \xi/2 > 0$, which means that the steady-state condition holds under the parameters of Table I.

Similarly to the case without RWA, we find the solution to the linearized QLEs. (29)-(30) in the frequency domain as

$$v(\omega) = [M - i\omega I_2]^{-1} L v_{\text{in}}(\omega). \quad (50)$$

Substituting Eq. (50) into the input-output relation $v_{\text{out}}(\omega) + v_{\text{in}}(\omega) = L v(\omega)$, we obtain

$$v_{\text{out}}(\omega) = X(\omega) v_{\text{in}}(\omega), \quad (51)$$

where the output field matrix $v_{\text{out}}(\omega)$ is the Fourier transform of $v_{\text{out}} = (\delta a_{\text{out}}, \delta b_{\text{out}})^T$. The scattering matrix for the symmetric optomechanical system can be written as

$$X(\omega) = L^T [M - i\omega I_2]^{-1} L - I_2. \quad (52)$$

The spectrum of the output field is defined as

$$s_{\text{out}}(\omega) = \int d\omega' \langle v_{\text{out}}^\dagger(\omega') v_{\text{out}}(\omega) \rangle. \quad (53)$$

Substituting Eq. (51) into Eq. (53), we find

$$s_{\text{out}}(\omega) = T(\omega) s_{\text{in}}(\omega), \quad (54)$$

where $T(\omega)$ is the contribution arising from the input laser field. The specific forms of the scattering probability can be expressed as

$$a \rightarrow b : T_a^b(\omega) = |X_a^b(\omega)|^2; a \leftarrow b : T_b^a(\omega) = |X_b^a(\omega)|^2. \quad (55)$$

In Sec. IV-B, we use the parameter values for the QED circuit in the Table I to carry out a numerical calculation to explore the conditions for the optimal reciprocal transmission of the incoming laser field. The QED circuit in Table I produces $\Delta_c'' = \Delta_m \approx 158\kappa_a = 158\gamma_b$. Here, we numerically verify the applicability of the RWA in this case. We here compare the scattering probability of a symmetric optomechanical system $P_a^b = P_b^a$ without RWA in Eqs. (46)-(47) and the one $T_a^b = T_b^a$ after RWA in Eq. (55).

In Fig. 5(a), we confirm that when the frequency of the input laser field satisfies the resonance condition $\omega = \Delta_c'' = \Delta_m$ and sideband resolved regime $\max(\kappa_a, \gamma_b) \ll \Delta_m$ for any effective optomechanical coupling we have $P_a^b \approx T_a^b$, that is, we can ignore the output spectrum resulting from the incoming optical vacuum field Θ_{vac}^a . Therefore, in Sec. IV-B, we can safely omit the non-resonant terms $\delta a \delta b$ and $\delta a^\dagger \delta b^\dagger$ using the RWA. In addition, Fig. 5(b) shows that with the enhancement of the effective optomechanical coupling G_R , the function Θ_{vac}^a becomes more and more obvious, eventually approaching 10^{-5} . After that, it exhibits robustness to G_R .

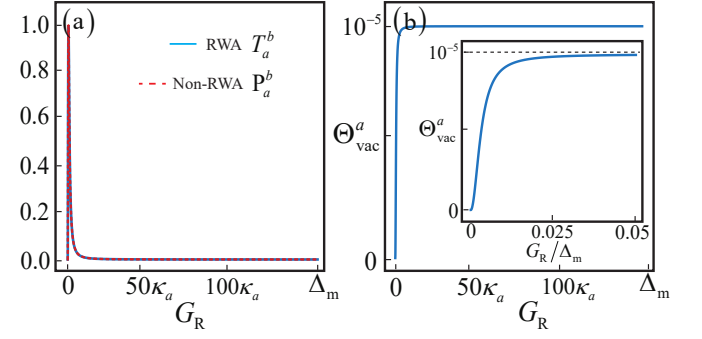


FIG. 5: (a) Scattering probabilities T_a^b after RWA (solid blue line) and P_a^b without RWA (orange dashed line) as functions of the effective optomechanical coupling $G_R \in [0, \Delta_m]$. (b) Output spectral contribution from the incoming optical vacuum field Θ_{vac}^a as a function of the effective optomechanical coupling $G_R \in [0, \Delta_m]$. The other parameters for (a) and (b) are chosen as $\omega = \Delta_c'' = \Delta_m = 158\kappa_a = 158\gamma_b$.

B. Critical points and optimal transmission condition

In this part, to ensure that the maximum scattering probability of the input laser field is unity under the parameter values for the QED circuit in Table I, we numerically calculate the scattering probability $T_a^b(\omega)$ from the optical mode a to the mechanical mode b after RWA to show the optimal reciprocal transmission in the symmetric optomechanics, which can be widely applied to the optical antenna and lossless isotropic materials [84]. Here, the symmetric optomechanics demands that the effective optomechanical coupling G_R is a real number. It is worth mentioning that for G to be a complex number, in our previous work [85], we have shown that in a three-mode optomechanical circulatory system, the complex angle difference of the different optomechanical couplings break the time-reversal symmetry, so that non-reciprocal transmission of the incoming laser field is achieved when the complex angle difference is equal to $\pm 0.5\pi + 2n\pi$ for $n = Z$.

Now, we focus on the numerical evaluation of the scattering probability $T_a^b(\omega)$ to show the optimal reciprocal transmission. The numerical results show the critical points and optimal condition for the observation of the optimal reciprocal transmission.

First, in Fig. 6, for $\kappa_a = \gamma_b \ll \Delta_m$, the scattering probability T_a^b is investigated as a function of the incoming laser frequency ω and the effective optomechanical coupling G_R . Figure 6 shows that the maximum value of $T_a^b(\omega)$ increases with G_R in a weakly coupled region $G_R < 0.5\kappa_a$. In particular, the optimal reciprocal transmission $T_a^b(\omega) = 1$ occurs for the first time at the strong-coupling critical point $G_R = 0.5\kappa_a$ when $\omega = \Delta_c'' = \Delta_m$, that is, the incoming laser frequency resonates with both the modified detuning frequency of the optical cavity field Δ_c'' and the mechanical detuning frequency Δ_m . In the strong coupling region $G_R > 0.5\kappa_a$, on the other hand, with enhancement of G_R , the single peak splits into two peaks, and the distance between the two symmetrical peaks become wider as G_R further increases. As G_R is further

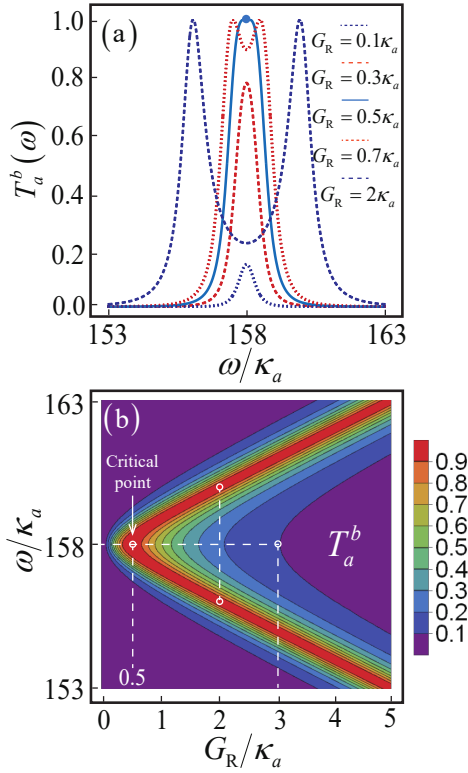


FIG. 6: The relation between the optimal reciprocal transmission of the incoming laser field and the effective optomechanical coupling G_R . (a) Scattering probability $T_a^b(\omega)$ from the optical mode a to the mechanical mode b as a functions of frequency of the incoming signal ω (in units of κ_a) for different values of effective optomechanical coupling: $G_R = 0.1\kappa_a$ (purple dotted line), $G_R = 0.3\kappa_a$ (orange dashed line), $G_R = 0.5\kappa_a$ (solid blue line), $G_R = 0.7\kappa_a$ (orange dotted line), $G_R = 2\kappa_a$ (purple dashed line). (b) Scattering probability T_a^b as a function of ω (in units of κ_a) and G_R (in units of κ_a). The other parameters for (a) and (b) are set to $\Delta_c'' = \Delta_m = 158\kappa_a = 158\gamma_b$.

strengthened, two symmetrical peaks for the optimal reciprocal transmission always appear with the resonant frequency $\omega = \Delta_c'' = \Delta_m$ being the axis of symmetry.

Then, we explore the influence of the environment on the optimal reciprocal transmission. In Fig. 7, we plot the scattering probability T_a^b as a function of the incoming laser frequency ω and the mechanical damping rate γ_b with the other parameters are set to $\Delta_c'' = \Delta_m = 158\kappa_a$ and $G_R = 0.5\kappa_a$. It is shown that for $\gamma_b < \kappa_a$, the maximum value of $T_a^b(\omega)$ increases as γ_b increases. In particular, we achieve the optimal reciprocal transmission when the dissipative balanced condition $\gamma_b = \kappa_a$ is satisfied. For $\gamma_b > \kappa_a$, as γ_b further increases, the maximum value of $T_a^b(\omega)$ gradually decreases, too. In addition, we observe that for $\gamma_b < \kappa_a$, the scattering probability $T_a^b(\omega)$ always presents a double peak with the resonant frequency $\omega = \Delta_c'' = \Delta_m$ being the axis of symmetry. With the further increase of γ_b , the scattering probability $T_a^b(\omega)$ presents a single peak at the resonant frequency $\omega = \Delta_c'' = \Delta_m$. Here, in contrast to Fig. 6, where T_a^b varies with G_R , we can see that T_a^b varies with γ_b in the opposite

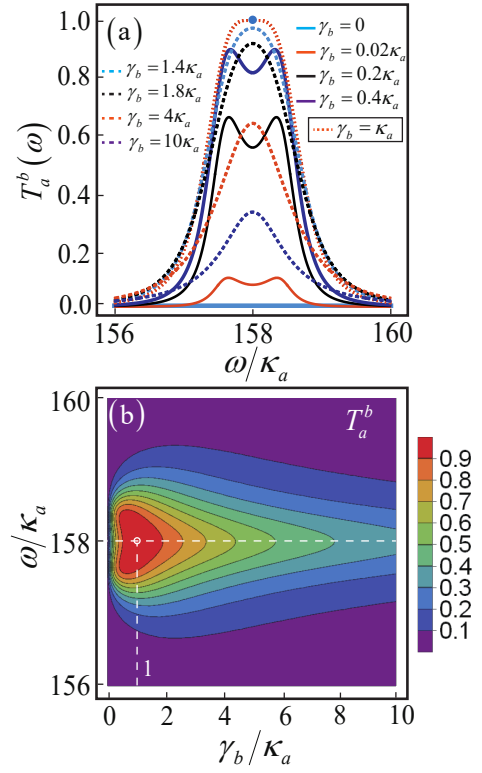


FIG. 7: The relation between the optimal reciprocal transmission of the incoming laser field and the mechanical damping rate γ_b . (a) The scattering probability $T_a^b(\omega)$ as functions of the frequency of the incoming signal ω (in units of κ_a) for different mechanical damping rates: $\gamma_b = 0$ (blue solid line), $\gamma_b = 0.02\kappa_a$ (orange solid line), $\gamma_b = 0.2\kappa_a$ (black solid line), $\gamma_b = 0.4\kappa_a$ (purple solid line), $\gamma_b = \kappa_a$ (orange dotted line), $\gamma_b = 1.4\kappa_a$ (blue dashed line), $\gamma_b = 1.8\kappa_a$ (black dashed line), $\gamma_b = 4\kappa_a$ (orange dashed line), $\gamma_b = 10\kappa_a$ (purple dashed line). The other parameters are set to $\Delta_c'' = \Delta_m = 158\kappa_a$ and $G_R = 0.5\kappa_a$. (b) Scattering probability T_a^b as a function of ω (in units of κ_a) and γ_b (in units of κ_a) with the other parameters are set to $\Delta_c'' = \Delta_m = 158\kappa_a$ and $G_R = 0.5\kappa_a$.

process. In short, the effective optomechanical coupling G_R promotes the splitting of the energy levels whereas the mechanical damping rate γ_b suppresses it.

Finally, considering all these factors, in Fig. 8, we plot the scattering probability T_a^b as a function of G_R and γ_b with the other parameters set to $\omega = \Delta_c'' = \Delta_m \gg \kappa_a = \gamma_b$. We are surprised to find that as long as the condition $G_R = 0.5\kappa_a$ is satisfied, the optimal reciprocal transmission always exists from an undamped optomechanical system to a strongly damped optomechanical system. Now, we analytically verify our numerical observation. In our case, if the parameters satisfy $\omega = \Delta_c'' = \Delta_m = \Delta \gg \kappa_a = \gamma_b = \xi$, the scattering matrix (52) can be cast into the following form:

$$\mathbf{X}(G_R, \xi) = \begin{bmatrix} \frac{0.5\xi^2}{0.25\xi^2 + G_R^2} - 1 & I \frac{\xi G_R}{0.25\xi^2 + G_R^2} \\ I \frac{\xi G_R}{0.25\xi^2 + G_R^2} & \frac{0.5\xi^2}{0.25\xi^2 + G_R^2} - 1 \end{bmatrix}. \quad (56)$$

The scattering probability $T(\omega)$ is given by $T(\omega) = |\mathbf{X}(G_R, \xi)|^2$. For $G_R = 0.5\xi$, the scattering matrix (56) re-

TABLE III: Summary of the results of our study on optimal reciprocal transmission: (a) optomechanical classification according to coupling type. (b) The relation between the optimal reciprocal transmission of the incoming laser field and the effective optomechanical coupling G_R . The other parameters are set to $\omega = \Delta_c'' = \Delta_m \gg \kappa_a = \gamma_b$. (c) The relation between the optimal reciprocal transmission of the incoming laser field and the mechanical damping rate γ_b . The other parameters are set to $\Delta_c'' = \Delta_m \gg \kappa_a$ and $G_R = 0.5\kappa_a$.

(a) Optomechanical type	Coupling	Dissipation	Frequency	Transmission Behavior
Standard optomechanics	$G \in C; G = 0.5\kappa_a$	$\gamma_b = \kappa_a$	$\Delta_c'' = \Delta_m$	Non-reciprocity [86, 87]
Symmetrical optomechanics	$G_R \in R; G_R = 0.5\kappa_a$	$\gamma_b = \kappa_a$	$\Delta_c'' = \Delta_m$	Reciprocity
(b) Real coupling	Max $T_a^b(G_R)$	Peak Number	Energy gap	$T_a^b(G_R) = 1$ points
$G_R < 0.5\kappa_a$	$G_R \uparrow T_a^b(G_R) \uparrow$	Single	N/A	Zero
$G_R = 0.5\kappa_a$	$T_a^b(G_R) \equiv 1$	Single	N/A	One
$G_R > 0.5\kappa_a$	$T_a^b(G_R) = 1$	Double	$G_R \uparrow \text{Gap} \uparrow$	Two
(c) Dissipation	Max $T_a^b(\gamma_b)$	Peak Number	Energy gap	$T_a^b(\gamma_b) = 1$ points
$\gamma_b < \kappa_a$	$\gamma_b \uparrow T_a^b(\gamma_b) \uparrow$	Double	$\gamma_b \uparrow \text{Gap} \uparrow$	Zero
$\gamma_b = \kappa_a$	$T_a^b(\gamma_b) \equiv 1$	Single	N/A	One
$\gamma_b > \kappa_a$	$\gamma_b \uparrow T_a^b(\gamma_b) \downarrow$	Single	N/A	Zero

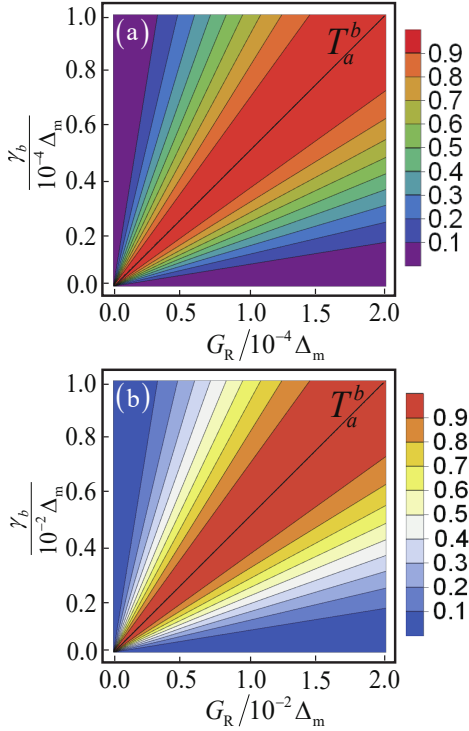


FIG. 8: Scattering probability T_a^b as a function of the effective optomechanical coupling G_R and the mechanical damping rate γ_b with the other parameters are set to $\omega = \Delta_c'' = \Delta_m \gg \kappa_a = \gamma_b$ and $G_R = 0.5\kappa_a$. (a) Case of weak dissipation: γ_b approaches $10^{-4}\Delta_m$. (b) Case of strong dissipation: γ_b approaches $10^{-2}\Delta_m$.

duces to $X(G_R = 0.5\xi) = [\{0, I\}, \{I, 0\}]$, and thus we find $T_a^b(G_R = 0.5\xi) = T_b^a(G_R = 0.5\xi) = 1$.

Finally, we summarize the results of our study on the optimal reciprocal transmission as follows; see Table III. The optimal reciprocal transmission needs to satisfy both of the

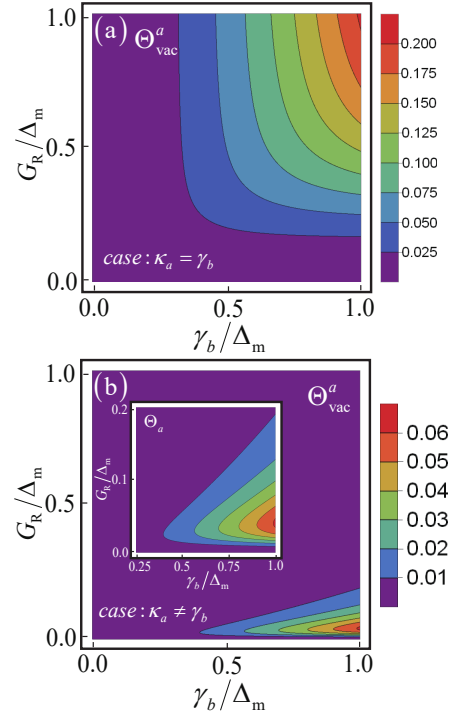


FIG. 9: Output spectral contribution from the incoming optical vacuum field Θ_{vac}^a as a function of the damping γ_b of the mechanical oscillator and the effective optomechanical coupling G_R . (a) Case of dissipative equilibrium: $\kappa_a = \gamma_b \in (0, \Delta_m)$. The other parameters are chosen as $\omega = \Delta_c'' = \Delta_m$ and $G_R \in (0, \Delta_m)$. (b) Case of dissipative non-equilibrium: $\kappa_a \neq \gamma_b \in (0, \Delta_m)$ with $\kappa_a = 1$. The other parameters are set to $\omega = \Delta_c'' = \Delta_m = 158\kappa_a$ and $G_R \in (0, \Delta_m)$.

following conditions: the incoming laser frequency ω resonates with both the modified detuning frequency of the optical cavity field Δ_c'' and the mechanical detuning frequency Δ_m ; the decay of the optical cavity κ_a is equal to the me-

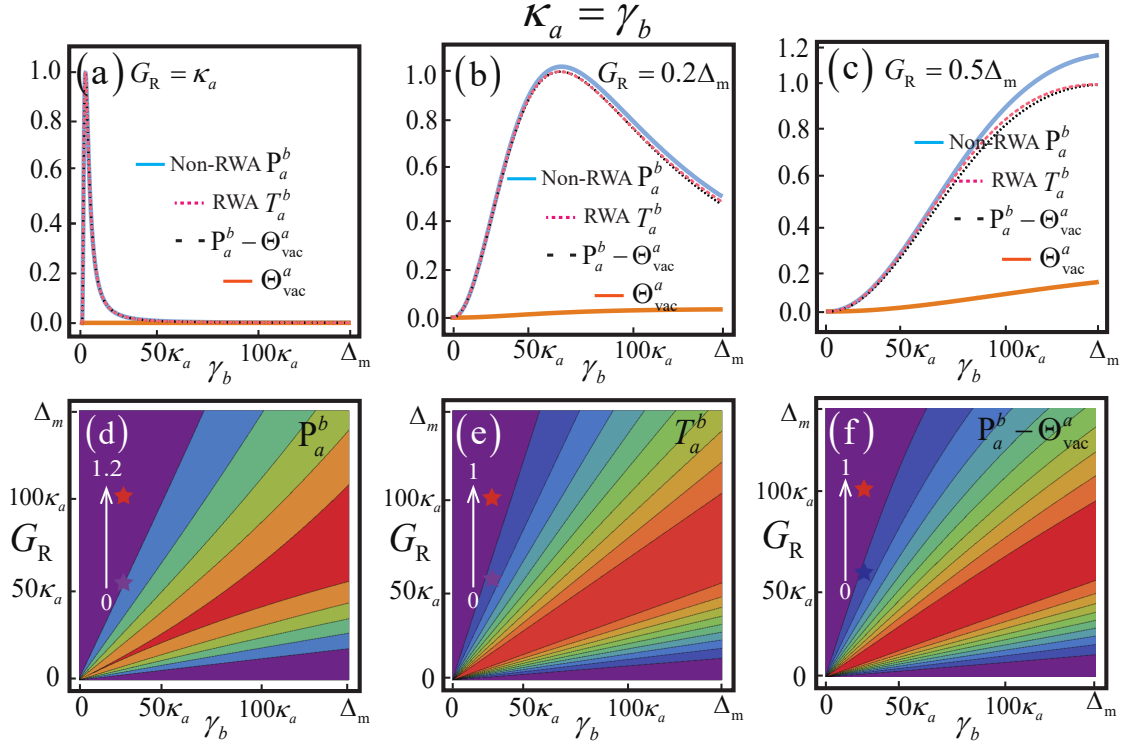


FIG. 10: Case of dissipative equilibrium: $\kappa_a = \gamma_b \in (0, \Delta_m)$. (a)-(c): We compare the scattering probabilities P_a^b before RWA and T_a^b after it as functions of the mechanical damping γ_b for different effective optomechanical coupling G_R : (a) $G_R = \kappa_a$, (b) $G_R = 0.2\Delta_m$, (c) $G_R = 0.5\Delta_m$. (d)-(f): Scattering probabilities P_a^b , T_a^b , and $P_a^b - \Theta_{vac}^a$ as functions of γ_b and different values of G_R . The other parameters are set to $\omega = \Delta_c'' = \Delta_m$ in (a)-(f).

chanical damping rate γ_b ; the optomechanical coupling G_R is equal to $0.5\kappa_a$. In addition, it is worth mentioning that for $G_R > 0.5\kappa_a$ and $\gamma_b = \kappa_a$, two symmetrical peaks for optimal reciprocal transmission always appear with the resonant frequency $\omega = \Delta_c'' = \Delta_m$ being the axis of symmetry. When $G_R > 3\kappa_a$ and $\gamma_b = \kappa_a$, the photon blocking effect is exhibited at the frequency resonance $\omega = \Delta_c'' = \Delta_m$, as we observe $T_a^b(\Delta_m) \approx 0$.

C. Non-RWA for dissipative equilibrium and non-equilibrium symmetric optomechanics

In this part, we consider the case of strong dissipation and ultrastrong coupling, in which the sideband resolved regime $\max(\kappa_a, \gamma_b) \ll \Delta_m$ is no longer met. Setting $\omega = \Delta_c'' = \Delta_m$ and $\max(\kappa_a, \gamma_b) \in (0, \Delta_m)$, we point out the contribution of the incoming optical vacuum field to the output spectrum Θ_{vac}^a , which is an effect of the anti-RWA terms, cannot always be neglected.

In Fig. 9, we plot Θ_{vac}^a as a function of the damping of the mechanical oscillator γ_b and the effective optomechanical coupling G_R . Figure 9(a) shows a case of dissipative equilibrium. We find that in the case of strong dissipation γ_b approaching Δ_m , the quantity Θ_{vac}^a continues to increase as G_R grows. In contrast to this, we give a case of dissipative non-

equilibrium in Fig. 9(b), in which there is a crossover region. When γ_b approaches Δ_m , with the increase of G_R , the quantity Θ_{vac}^a first increases, and then decreases.

In the dissipative equilibrium case $\kappa_a = \gamma_b \in (0, \Delta_m)$, in Fig. 10(a)-(c), we compare the scattering probabilities P_a^b before RWA and T_a^b after it as functions of γ_b for different values of G_R . To be specific, when $G_R = \kappa_a$, we can see that $P_a^b \approx T_a^b$. It is also shown that for $G_R = \kappa_a$ as the increase of γ_b , the scattering probabilities initially increases and then decreases. When $G_R = 0.2\Delta_m$ and $G_R = 0.5\Delta_m$, we have $P_a^b > T_a^b$. We numerically find that the approximate relation $P_a^b - \Theta_{vac}^a \approx T_a^b$ always hold, which means that the difference between the non-RWA and the RWA cases is due to the contribution of the input vacuum field, Θ_{vac}^a . We also find that for $G_R = 0.5\Delta_m$ with the increase of γ_b , the scattering probabilities continues to increase. In Fig. 10(d)-(f), we plot the scattering probabilities P_a^b , T_a^b , and $P_a^b - \Theta_{vac}^a$ as functions of γ_b and different values of G_R with parameters $\omega = \Delta_c'' = \Delta_m$ and $\kappa_a = \gamma_b \in (0, \Delta_m)$. We find that the result in Fig. 10(a)-(f) is consistent with that in Fig. 9(a).

Similarly, in the dissipative non-equilibrium case: $\kappa_a \neq \gamma_b \in (0, \Delta_m)$ with $\kappa_a = 1$, we also numerically find that the approximate relation $P_a^b - \Theta_{vac}^a \approx T_a^b$ always hold. We show that the result in Fig. 11 is consistent with that in Fig. 9(b). The significant difference between Fig. 10(b) and Fig. 11(c) in the ultrastrong region is that in the case of dissipative equi-

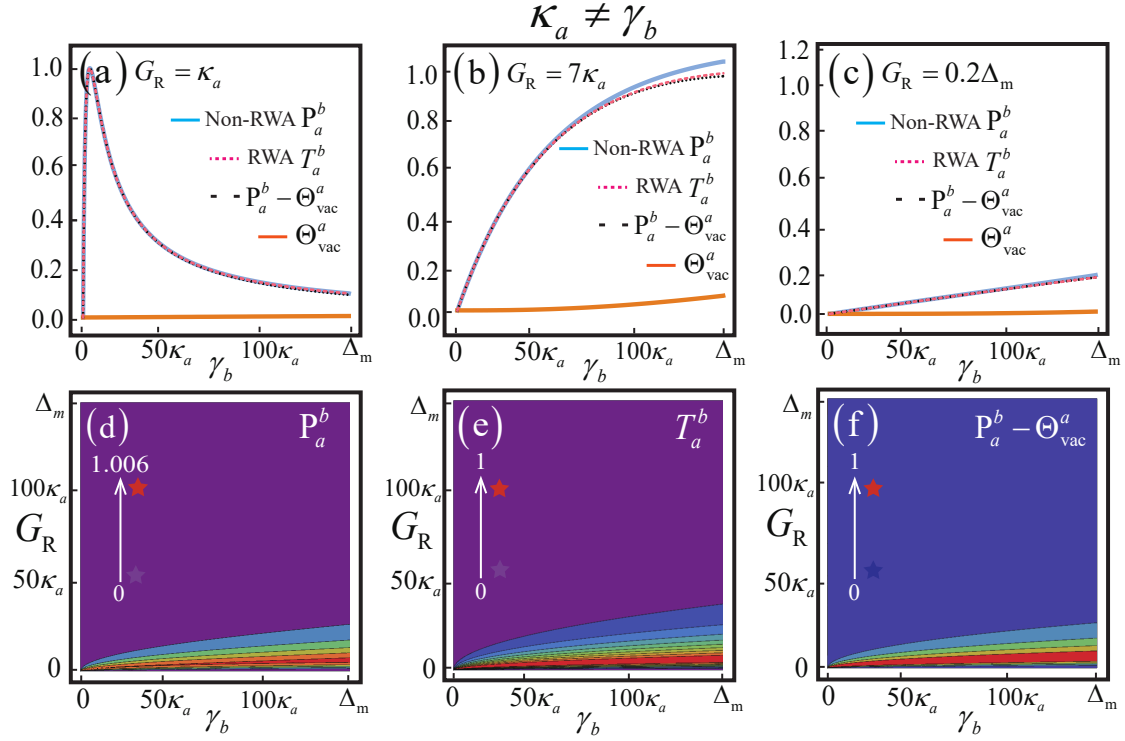


FIG. 11: Case of dissipative non-equilibrium: $\kappa_a \neq \gamma_b \in (0, \Delta_m)$ with $\kappa_a = 1$. (a)-(c): We compare the scattering probabilities $P_a^b(\gamma_b)$ before RWA and $T_a^b(\gamma_b)$ after it as functions of γ_b for different values of G_R : (a) $G_R = \kappa_a$, (b) $G_R = 7\kappa_a$, (c) $G_R = 0.2\Delta_m$. (d)-(f): Scattering probabilities P_a^b , T_a^b , and $P_a^b - \Theta_{\text{vac}}^a$ as functions of γ_b and different values of G_R . The other parameters are set to $\omega = \Delta_c'' = \Delta_m = 158\kappa_a$ in (a)-(f).

librium, the scattering probabilities first increases rapidly and then decreases with the increase of γ_b , while in the case of dissipative non-equilibrium, the scattering probabilities continues to grow very slowly with the increase of γ_b .

In summary, we have discussed the effect of dissipation on laser signal transmission in a symmetrical optomechanical system. More importantly, we modify the expression of scattering probability under the non-RWA. Further, we numerically find that the approximate relation $P_a^b - \Theta_{\text{vac}}^a \approx T_a^b$ always hold.

V. EXPERIMENTAL IMPLEMENTATION

We may be able to materialize the present theoretical model in circuit quantum electrodynamics (QED) experiments [88, 89]. As shown in Fig. 12, we propose the QED device that consists of three parts made with patterned thin films of superconducting aluminum on a silicon chip. The first part is a microwave resonator, namely, an optical cavity (green), the second part is a micromechanical resonator (blue), and the third is a charge quantum two-level system, namely, a qubit (orange), which consists of small Josephson tunnel junctions and mediates an interaction between the former two parts.

One of the motivations for this work is to obtain a controllable nonlinear coupling consisting of two parts. One is

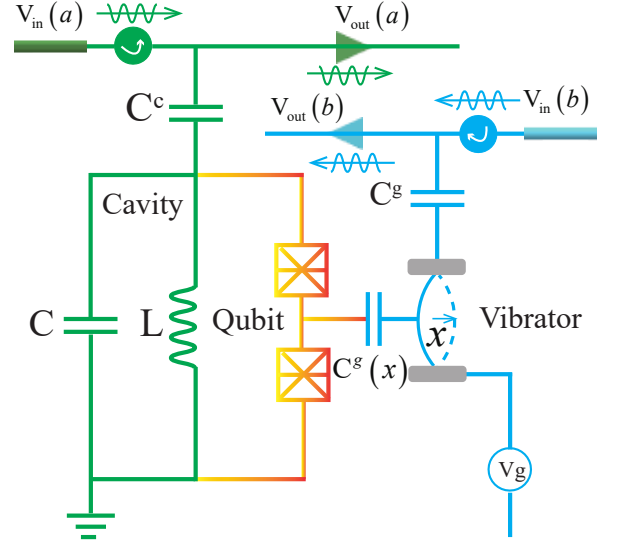


FIG. 12: (Color online) QED-circuit realization of symmetric optomechanics. This experimental setup is made of a qubit (orange) coupled to an on-chip cavity (green) and a nano-mechanical resonator (blue).

the intrinsic nonlinear pressure coupling in single-photon optomechanics, which is originated from the momentum transfer of one photon. Since only one photon exists, the radiation-

pressure force caused by the photon momentum transfer is extremely weak. The point of the device is how to generate the CK nonlinear coupling, thereby enhancing the optomechanical radiation-pressure nonlinearity. Usually, when two electric fields are applied simultaneously on a Kerr nonlinear medium, the CK effect can occur. In this device, the generation of the CK nonlinearity is divided into three steps. First, an extensive DC voltage bias V_g applied to the mechanical resonator is represented as a movable capacitance $C_g(x)$. Second, the mechanical resonator and the qubit produce a longitudinal coupling in the natural basis of the charge qubit and result in the most significant impact on the energy of the qubit through the mechanical resonator. Third, the transverse interaction between the qubit and the optical cavity makes latter experience a Stark shift. This Stark shift contains a contribution from the vibrations due to their effect on the qubit level spacing [90]. Through the above procedure, the nonlinear coupling between the mechanical and optical modes can be amplified in this setting by a factor of the order of $CV_g/2e$, which is up to six orders of magnitude for a typical experiment [91]. More importantly, the damping of the mechanics becomes affected by the nonlinearities. Based on the above analysis, the QED-circuit is a potential platform of the present theory.

VI. SUMMARY AND PROSPECT

In summary, based on the CK interaction, we have proposed a reliable scheme to realize controllable enhancement of the single-photon optomechanical coupling. We have proposed effective symmetric optomechanics at a single-photon level, in which the forms of the quantum fluctuation dynamics satisfied by the photon and the phonon are identical. Then we have shown the optimal reciprocal transport in this symmetric optomechanics. By observing the critical behavior of the optimal transmission of the laser field, we have identified the boundary point of the optomechanical strong coupling. We have compared the scattering behavior of the laser field in the dissipative equilibrium and non-equilibrium symmetric optomechanics before and after the RWA. We note that a QED circuit can implement symmetric optomechanics. This work may pave the way to studying the single-photon optomechanical effects with current experimental platforms.

This work also reveals how the form of optomechanical coupling and the type of dissipation affect the scattering characteristics of the input laser signal in an open quantum system. Further, we can explore the influence of optomechanical coupling and dissipation on optomechanical-induced transparency [92–94] and negative entanglement [95–97] in open quantum systems.

VII. ACKNOWLEDGMENTS

The author is grateful to Naomichi Hatano for fruitful discussions and for carefully proofreading the manuscript.

The author also thanks Yue-Zhou Li and Hongchao Li for their valuable comments. Cheng Shang is supported by the China Scholarship Council and the Japanese Government (Monbukagakusho-MEXT) Scholarship under Grant No. 211501.

Appendix A: Details of the derivation of Eq. (1)

Here, we show the origin of the generalized optomechanical model H_{FP} from a decoupled cavity optomechanics [41–44]. To begin with, let us consider an optomechanical system without interactions. Considering the limitation of optomechanical experiments, we set the Hamiltonian for an uncoupled optomechanical system in the simple form

$$H_A = \hbar\omega_c a^\dagger a + \hbar\omega_m b^\dagger b, \quad (\text{A1})$$

where a^\dagger (a) and b^\dagger (b) are the creation (annihilation) operators of the optical and mechanical modes with the corresponding resonance frequencies ω_c and ω_m , respectively.

Then we assume that the movable mirror works with a slight mechanical motion. Thus, the resonance frequency of the optical cavity is modulated by the mechanical amplitude. In the present paper, we keep only the contributions of the linear and first nonlinear terms in the Taylor expansion:

$$\omega_c(x) = \omega_c + x \frac{\partial\omega_c(x)}{\partial x} + \frac{1}{2}x^2 \frac{\partial^2\omega_c(x)}{\partial x^2} + \dots \quad (\text{A2})$$

Here, $x = x_{\text{ZPF}}(b^\dagger + b)$, where x_{ZPF} is the amplitude of the zero-point fluctuation of the mechanical oscillator, while $-\partial\omega_c(x)/\partial x$ is the shift of the optical frequency per displacement. Now, we define g_0 and χ as follows:

$$g_0 = -x_{\text{ZPF}} \frac{\partial\omega_c(x)}{\partial x}, \quad \chi = x_{\text{ZPF}}^2 \frac{\partial^2\omega_c(x)}{\partial x^2}, \quad (\text{A3})$$

where g_0 and χ are often known as the single-photon optomechanical coupling and the cross-Kerr coupling, respectively. Hence, Eq. (A2) can be rewritten as

$$\omega_c(x) = \omega_c - g_0(b^\dagger + b) + \frac{1}{2}\chi(b^\dagger + b)^2 + \text{O}(x^3). \quad (\text{A4})$$

We further simplify Eq. (A4) by invoking the rotating-wave approximation, in which we omit the non-resonant terms $b^\dagger b^\dagger$ and bb in the sideband resolved and red detuned regimes [79, 80]. Substituting the result into Eq. (A1), we find Eq. (1) in the main text: $H_{\text{FP}} = \hbar\omega_c a^\dagger a + \hbar\omega_m b^\dagger b - \hbar g_0 a^\dagger (b^\dagger + b) + \hbar\chi a^\dagger a b^\dagger b$. Physically, the radiation-pressure interaction g_0 represents the frequency shift of the optical cavity field, which depends on the displacement of the mechanical resonator from the equilibrium position. The cross-Kerr interaction χ is interpreted as a change in the reflective index of the optical cavity field, which depends on the number of mechanical phonons.

Appendix B: Details of the derivation of Eq. (9) and β_s

In this Appendix, we derive the nonlinear quantum Langevin equations that the final enhanced Hamiltonian H_T satisfies [57]. Let us focus on the mechanical mode as an example; Eq. (8) for the optical cavity mode is derived similarly. The Heisenberg equations of motion for the system operator b and its corresponding reservoir operators Γ_{bk} are given by

$$\dot{b} = -i\Delta_m b + ig_s a^\dagger a - i(\Omega_b - \beta_s \Delta_m) - i \sum_k g_{bk} \Gamma_{bk}, \quad (\text{B1})$$

$$\dot{\Gamma}_{bk} = -i\omega_{bk} \Gamma_{bk} - ig_{bk} (b - \beta_s). \quad (\text{B2})$$

We are interested in a closed equation for the system operator b . Equation (B2) for the reservoir operator Γ_{bk} can be formally integrated to yield

$$\Gamma_{bk}(t) = +\Gamma_{bk}(t_0) e^{-i\omega_{bk}(t-t_0)} - ig_{bk} \int_{t_0}^t d\tau [b(\tau) - \beta_s] e^{-i\omega_{bk}(t-\tau)}. \quad (\text{B3})$$

Here the first term describes the free evolution of the reservoir modes, whereas the second term arises from their interaction with the mechanical mode. We eliminate the reservoir operators Γ_{bk} by substituting Eq. (B3) into Eq. (B1), finding

$$\begin{aligned} \dot{b} = & -i\Delta_m b + ig_s a^\dagger a - i(\Omega_b - \beta_s \Delta_m) \\ & - \sum_k g_{bk}^2 \int_{t_0}^t d\tau [b(\tau) - \beta_s] e^{-i\omega_{bk}(t-\tau)} \\ & - i \sum_k g_{bk} \Gamma_{bk}(t_0) e^{-i\omega_{bk}(t-t_0)}. \end{aligned} \quad (\text{B4})$$

In Eq. (B4), we can see that the evolution of the system operator depends on the fluctuations in the reservoir. Next, we make some approximations. As in the Weisskopf-Wigner approximation [58], we consider the spectrum to be given by the normal modes of a large scale, and these modes are very close in frequency. We then approximate this spectrum by a continuous spectrum. Thus, the summation in Eq. (B4) can be written as

$$\begin{aligned} \dot{b} = & -i\Delta_m b + ig_s a^\dagger a - i(\Omega_b - \beta_s \Delta_m) \\ & - i \int_0^{+\infty} g_b(\omega_b) \frac{d\kappa(\omega_b)}{d\omega_b} \Gamma_b(\omega_b, t_0) e^{-i\omega_b(t-t_0)} d\omega_b \\ & - \int_{t_0}^t \int_0^{+\infty} g_b^2(\omega_b) \frac{d\kappa(\omega_b)}{d\omega_b} [b(\tau) - \beta_s] e^{-i\omega_b(t-\tau)} d\omega_b d\tau. \end{aligned} \quad (\text{B5})$$

Considering an ideal situation, we assume for simplicity that $[g_b(\omega_b)]^2 d\kappa(\omega_b)/d\omega_b = \gamma_b/2\pi > 0$ is constant, so that Eq. (B5) is reduced to a simple first-order differential equation [59]:

$$\begin{aligned} \dot{b} = & -i\Delta_m b + ig_s a^\dagger a - i(\Omega_b - \beta_s \Delta_m) \\ & - i\sqrt{\frac{\gamma_b}{2\pi}} \int_0^{+\infty} \Gamma_b(\omega_b, t_0) e^{-i\omega_b(t-t_0)} d\omega_b \\ & - \frac{\gamma_b}{2\pi} \int_{t_0}^t \int_0^{+\infty} [b(\tau) - \beta_s] e^{-i\omega_b(t-\tau)} d\omega_b d\tau. \end{aligned} \quad (\text{B6})$$

Using the relation

$$\int_0^{+\infty} d\omega_b e^{-i\omega_b(t-\tau)} = \pi \delta(t-\tau), \quad (\text{B7})$$

we arrive at Eq. (8) in the main text:

$$\dot{b} = -\left(i\Delta_m + \frac{\gamma_b}{2}\right)b + ig_s a^\dagger a + \sqrt{\gamma_b} b_{\text{in}} + \dot{\beta}_s \quad (\text{B8})$$

with

$$\begin{aligned} b_{\text{in}}(t) &= -\frac{i}{\sqrt{2\pi}} \int_0^{+\infty} \Gamma_b(\omega_b, t_0) e^{-i\omega_b(t-t_0)} d\omega_b, \\ \dot{\beta}_s &= \frac{\gamma_b}{2} \beta_s - i(\Omega_b - \beta_s \Delta_m) = 0, \end{aligned} \quad (\text{B9})$$

where b_{in} is a noise operator which depends upon the initial-time environment operators $\Gamma_b(\omega_b, t_0)$, while γ_b is the mechanical damping rate which depends on the coupling strength g_{bk} of the system and the reservoir. This produces Eq. (9) in the main text. The same holds true for Eq. (8).

Appendix C: An alternative viewpoint on the selection of β_s

In this Appendix, we present the physical meaning of the coherent displacement amplitude β at a steady state from the point of view of the Gorini-Kossakowski-Sudarshan-Lindblad (GKSL) equation [57, 58]. The derivation here is based on a recent related work [56]. To begin with, let us consider an optical mode a and a mechanical mode b which are coupled to two individual Markovian heat baths consisting of assemblies of the oscillators. When the reservoir modes Γ_{ak} and Γ_{bk} are initially in the thermal equilibrium, in the presence of dissipations, the evolution of the field system ρ_S is governed by the GKSL master equation as follows:

$$\begin{aligned} \dot{\rho}_S = & \frac{i}{\hbar} [\rho_S, H_S^P] + \kappa_a (\bar{n}_a + 1) L[a] \rho_S + \kappa_a \bar{n}_a L[a^\dagger] \rho_S \\ & + \gamma_b (\bar{n}_b + 1) L[b] \rho_S + \gamma_b \bar{n}_b L[b^\dagger] \rho_S, \end{aligned} \quad (\text{C1})$$

where the standard Lindblad superoperator for the optical mode damping can be written as $L[a] \rho_S = a \rho_S a - (a^\dagger a \rho_S + \rho_S a^\dagger a)$, and the same goes for the mechanical mode damping. Here, ρ_S denotes the reduced density operator for the open system (3), \bar{n}_a and \bar{n}_b denote the number operators of the reservoirs corresponding to the optical mode a and mechanical mode b , respectively, κ_a denotes the decay rate of the optical cavity and γ_b denotes the mechanical damping rate.

When a high-power laser drives the mechanical mode, we can make the following displacement transformation in the coherent-state representation:

$$\rho'_S = D(\beta) \rho_S D^\dagger(\beta), \quad (\text{C2})$$

where ρ'_S is the reduced density operator for the closed system H_S^P in the displacement representation. In the displacement operator $D(\beta) = \exp(\beta b^\dagger - \beta^* b)$, β is the amplitude of the

coherent displacement, which needs to be determined in the transformed master equation.

We now try to find the GKSL master equation for ρ'_S . The time derivative of Eq. (C2) reads

$$\dot{\rho}'_S = \dot{D}(\beta) \rho_S D^\dagger(\beta) + D(\beta) \dot{\rho}_S D^\dagger(\beta) + D(\beta) \rho_S \dot{D}^\dagger(\beta) \quad (C3)$$

Using the relations $D(\beta) D^\dagger(\beta) = I$ and $D(\beta) = \exp(\beta \beta^*/2) \exp(-b \beta^*) \exp(b^\dagger \beta)$, we find $\dot{D}(\beta)$ and $\dot{D}^\dagger(\beta)$ as in

$$\dot{D}(\beta) = \frac{1}{2} (\dot{\beta} \beta^* - \beta \dot{\beta}^*) D(\beta) + D(\beta) (\dot{\beta} b^\dagger - \dot{\beta}^* b), \quad (C4)$$

$$\dot{D}^\dagger(\beta) = -\frac{1}{2} (\dot{\beta} \beta^* - \beta \dot{\beta}^*) D^\dagger(\beta) + (\dot{\beta}^* b - \dot{\beta} b^\dagger) D^\dagger(\beta).$$

We can thereby reduce Eq. (C3) to

$$\dot{\rho}'_S = D(\beta) \dot{\rho}_S D^\dagger(\beta) - D(\beta) [\rho_S, (\dot{\beta} b^\dagger - \dot{\beta}^* b)] D^\dagger(\beta) \quad (C5)$$

Using the expressions $D(\beta) b D^\dagger(\beta) = b - \beta$ and $D(\beta) b^\dagger D^\dagger(\beta) = b^\dagger - \beta^*$ and inserting Eq. (C1) into Eq. (C5), we find the transformed GKSL master equation in the form

$$\begin{aligned} \dot{\rho}'_S = & \frac{i}{\hbar} [\rho'_S, H_S^{P'}] + \kappa_a (\bar{n}_a + 1) L[a] \rho'_S + \kappa_a \bar{n}_a L[a^\dagger] \rho'_S \\ & + \gamma_b (\bar{n}_m + 1) L[b] \rho'_S + \gamma_b \bar{n}_m L[b^\dagger] \rho'_S \\ & + \left[\dot{\beta} + \left(i\Delta_m + \frac{\gamma_b}{2} \right) \beta - i\Omega_b \right] [b^\dagger, \rho'_S] \\ & - \left[\dot{\beta}^* + \left(-i\Delta_m + \frac{\gamma_b}{2} \right) \beta^* + i\Omega_b^* \right] [b, \rho'_S], \end{aligned} \quad (C6)$$

where

$$\begin{aligned} H_S^{P'} = & +\hbar [\Delta_c + \chi|\beta|^2 + 2g_0 \text{Re}(\beta)] a^\dagger a \\ & +\hbar (\Delta_m + \chi a^\dagger a) b^\dagger b - \hbar \chi a^\dagger a (\beta b^\dagger + \beta^* b) \\ & -\hbar g_0 a^\dagger a (b^\dagger + b) + \hbar \Omega_a^* a + \hbar \Omega_a a^\dagger. \end{aligned} \quad (C7)$$

We can see that the condition for the GKSL master equation to remain unchanged after the coherent displacement transformation is

$$\dot{\beta}(t) + \left(i\Delta_m + \frac{\gamma_b}{2} \right) \beta(t) - i\Omega_b = 0. \quad (C8)$$

By solving Eq. (C8), we obtain the solution of the amplitude of the transient displacement as follows:

$$\beta(t) = \frac{\Omega_b}{\Delta_m - i0.5\gamma_b} + C(t_0) e^{-(i\Delta_m + 0.5\gamma_b)t}, \quad (C9)$$

In the limit $t \rightarrow +\infty$, the amplitude is reduced to the steady-state solution

$$\beta_s = \frac{\Omega_b}{\Delta_m - i0.5\gamma_b}. \quad (C10)$$

We can see from Eq. (C10) that the amplitude of steady-state coherent displacement β_s is tunable by choosing proper parameters Ω_b and Δ_m .

Then, taking β_s , we obtain the GKSL master equation in the displacement representation as in

$$\begin{aligned} \dot{\rho}'_S = & \frac{i}{\hbar} [\rho'_S, H_S^{P''}] + \kappa_a (\bar{n}_a + 1) L[a] \rho'_S + \kappa_a \bar{n}_a L[a^\dagger] \rho'_S \\ & + \gamma_b (\bar{n}_m + 1) L[b] \rho'_S + \gamma_b \bar{n}_m L[b^\dagger] \rho'_S, \end{aligned} \quad (C11)$$

for which the steady-state transformed Hamiltonian in the displacement representation becomes

$$\begin{aligned} H_S^{P''} = & +\hbar \Delta_c^0 a^\dagger a + \hbar (\Delta_m + \chi a^\dagger a) b^\dagger b \\ & -\hbar a^\dagger a (g_s b^\dagger + g_s^* b) + \hbar \Omega_a^* a + \hbar \Omega_a a^\dagger \end{aligned} \quad (C12)$$

with $\Delta_c^0 = \Delta_c + \chi|\beta_s|^2$ being the normalized optical cavity detuning including the frequency shift caused by the high-power laser driving and $g_s = \chi\beta_s$. Since our motivation is to study the few-photon physics in strong optomechanical system, we demand the constraint condition $\chi \approx 10^{-3} \Delta_m$ in circuit-QED [50–52, 56]. Thus we neglect the CK interaction term in Eq. (C12) to obtain the approximation Hamiltonian: $H_S^{\text{app}} = \hbar \Delta_c^0 a^\dagger a + \hbar \Delta_m b^\dagger b - \hbar a^\dagger a (g_s b^\dagger + g_s^* b) + \hbar \Omega_a^* a + \hbar \Omega_a a^\dagger$.

Appendix D: Scattering Probability modification for non-RWA case with ultratrong coupling

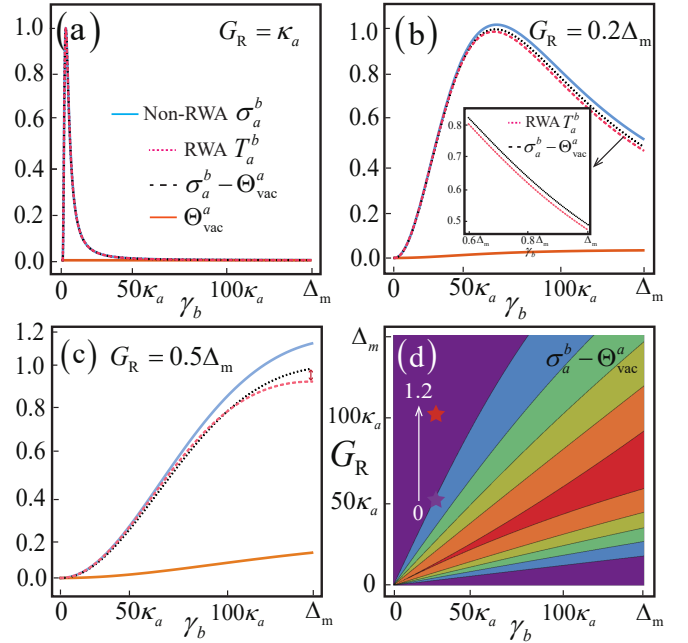


FIG. 13: We compare the scattering probabilities σ_a^b before the RWA in Eq. (D1) and T_a^b after it as functions of the mechanical damping γ_b for different effective optomechanical coupling G_R : (a) $G_R = \kappa_a$, (b) $G_R = 0.2\Delta_m$, (c) $G_R = 0.5\Delta_m$. We show the scattering probability $\sigma_a^b - \Theta_{\text{vac}}^a$ as a function of G_R and γ_b in (d). The other parameters are set to $\kappa_a = \gamma_b \in (0, \Delta_m)$ and $\omega = \Delta_c' = \Delta_m$.

In this Appendix, we prove numerically that Eq. (46) is more universal than the results in Ref. [81] for non-RWA

cases after a slight modification. The expression of the scattering probability in Ref. [81] is only successful in the cases of weak coupling and strong coupling. However, in the case of ultrastrong coupling, it needs to be modified to Eq. (46).

The numerical validation process is as follows. In the non-RWA case, the scattering probability from a to b described in Ref. [81] is

$$\sigma_a^b(\omega) = |O_a^b(\omega)|^2 + |O_a^{b\dagger}(\omega)|^2. \quad (D1)$$

Using the same values of parameters as in Fig. 10(a)-(c),

we use Eq. (D1) to numerically calculate the scattering probability of input signal from weak coupling to ultrastrong coupling cases in Fig. 13(a)-(c). When $G_R = \kappa_a$, the equality $\sigma_a^b - \Theta_{\text{vac}}^a = T_a^b$ is always true, which is consistent with the cases of weak coupling and strong coupling discussed in Ref. [81]. However, in the ultrastrong coupling case, when $G_R = 0.2\Delta_m$ and $G_R = 0.5\Delta_m$, under strong dissipation, $\max(\sigma_a^b - \Theta_{\text{vac}}^a) > \max(T_a^b) = 1$, which violates the law of conservation of energy [98, 99]. Compared with it, Eq. (46) satisfies $P_a^b - \Theta_{\text{vac}}^a = T_a^b$ under any coupling strength; see Fig. 10.

-
- [1] M. Aspelmeyer, T. J. Kippenberg, and F. Marquardt, *Cavity Optomechanics: Nano- and Micromechanical Resonators Interacting with Light* (Springer, Germany, 2014).
 - [2] M. Aspelmeyer, T. J. Kippenberg, and F. Marquardt, Cavity optomechanics, *Rev. Mod. Phys.* **86**, 1391 (2014).
 - [3] W. P. Bowen and G. J. Milburn, *Quantum optomechanics* (CRC, USA, 2016).
 - [4] T. J. Kippenberg and K. J. Vahala, Cavity optomechanics: Back-action at the mesoscale, *Science* **321**, 1172 (2008).
 - [5] F. Marquardt and S. M. Girvin, Optomechanics, *Physics* **2**, 40 (2009).
 - [6] M. Aspelmeyer, P. Meystre, and K. Schwab, Quantum optomechanics, *Phys. Today* **65**(7), 29 (2012).
 - [7] A. Nunnenkamp, K. Børkje, and S. M. Girvin, Single-Photon Optomechanics, *Phys. Rev. Lett.* **107**, 063602 (2011).
 - [8] T. Hong, H. Miao, and Y. Chen, Open quantum dynamics of single-photon optomechanical devices, *Phys. Rev. A* **88**, 023812 (2013).
 - [9] H. X. Tang and D. Vitali, Prospect of detecting single-photon-force effects in cavity optomechanics, *Phys. Rev. A* **89**, 063821 (2014).
 - [10] J.-Q. Liao, H. K. Cheung, and C. K. Law, Spectrum of single-photon emission and scattering in cavity optomechanics, *Phys. Rev. A* **85**, 025803 (2012).
 - [11] P. Rabl, Photon Blockade Effect in Optomechanical Systems, *Phys. Rev. Lett.* **107**, 063601 (2011).
 - [12] J.-Q. Liao and F. Nori, Photon blockade in quadratically coupled optomechanical devices, *Phys. Rev. A* **88**, 023853 (2013).
 - [13] H. Z. Shen, Cheng Shang, Y. H. Zhou, and X. X. Yi, Unconventional single-photon blockade in non-Markovian systems, *Phys. Rev. A* **98**, 023856 (2018).
 - [14] H. Y. Sun, Cheng Shang, X. X. Luo, Y. H. Zhou, and H. Z. Shen, Optical-assisted Photon Blockade in a Cavity System via Parametric Interactions, *Int. J. Theor. Phys.* **58**, 3640 (2019).
 - [15] J.-Q. Liao and L. Tian, Macroscopic Quantum Superposition in Cavity Optomechanics, *Phys. Rev. Lett.* **116**, 163602 (2016).
 - [16] W. Marshall, C. Simon, R. Penrose, and D. Bouwmeester, Towards Quantum Superpositions of a Mirror, *Phys. Rev. Lett.* **91**, 130401 (2003).
 - [17] Max Ludwig, B. Kubala, and F. Marquardt, The optomechanical instability in the quantum regime, *New J. Phys.* **10**, 095013 (2008).
 - [18] F. Brennecke, S. Ritter, T. Donner, and T. Esslinger, Cavity Optomechanics with a Bose-Einstein Condensate, *Science* **322**, 235 (2008).
 - [19] A. Xuereb, C. Genes, and A. Dantan, Strong Coupling and Long-Range Collective Interactions in Optomechanical Arrays, *Phys. Rev. Lett.* **109**, 223601 (2012).
 - [20] T. P. Purdy, P.-L. Yu, R. W. Peterson, N. S. KaMPeL, and C. A. Regal, Strong Optomechanical Squeezing of Light, *Phys. Rev. X* **3**, 031012 (2013).
 - [21] X.-Y. Lü, Y. Wu, J. R. Johansson, H. Jing, J. Zhang, and F. Nori, Squeezed Optomechanics with Phase-Matched Amplification and Dissipation, *Phys. Rev. Lett.* **114**, 093602 (2015).
 - [22] M.-A. Lemonde, N. Didier, and A. A. Clerk, Enhanced nonlinear interactions in quantum optomechanics via mechanical amplification, *Nat. Commun.* **7**, 11338 (2016).
 - [23] Z. Y. Wang and A. H. S.-Naeini, Enhancing a slow and weak optomechanical nonlinearity with delayed quantum feedback, *Nat. Commun.* **8**, 15886 (2017).
 - [24] W. Xiong, J. J. Chen, B. L. Fang, M. F. Wang, L. Ye, and J. Q. You, Strong tunable spin-spin interaction in a weakly coupled nitrogen vacancy spin-cavity electromechanical system, *Phys. Rev. B* **103**, 174106 (2021).
 - [25] X.-L. Yin, Y.-H. Zhou, and J.-Q. Liao, All-optical quantum simulation of ultrastrong optomechanics, *Phys. Rev. A* **105**, 013504 (2022).
 - [26] I. Söllner, L. Midolo, and P. Lodahl, Deterministic Single-Phonon Source Triggered by a Single Photon, *Phys. Rev. Lett.* **116**, 234301 (2016).
 - [27] R. Khan, F. Massel, T. T. Heikkilä, Cross-Kerr nonlinearity in optomechanical systems, *Phys. Rev. A* **91**, 043822 (2015).
 - [28] S. Ding, G. Maslennikov, R. Hablütze, and D. Matsukevich, Cross-Kerr Nonlinearity for Phonon Counting, *Phys. Rev. Lett.* **119**, 193602 (2017).
 - [29] C. K. Law, Effective Hamiltonian for the radiation in a cavity with a moving mirror and a time-varying dielectric medium, *Phys. Rev. A* **49**, 433 (1994).
 - [30] R. Sarala, F. Massel, Cross-Kerr nonlinearity: a stability analysis, *Nanoscale Systems: Mathematical Modeling, Theory and Application*, **4**(1), 2299 (2015).
 - [31] F. Zhou, L. B. Fan, J.-F. Huang, and J.-Q. Liao, Enhancement of few-photon optomechanical effects with cross-Kerr nonlinearity, *Phys. Rev. A* **99**, 043837 (2019).
 - [32] M. A. Lemonde, N. Didier, and A. A. Clerk, Nonlinear Interaction Effects in a Strongly Driven Optomechanical Cavity, *Phys. Rev. Lett.* **111**, 053602 (2013).
 - [33] J.-S. Zhang, M.-C. Li, and A.-X. Chen, Enhancing quadratic optomechanical coupling via a nonlinear medium and lasers, *Phys. Rev. A* **99**, 013843 (2019).
 - [34] S. Chakraborty and A. K. Sarma, Enhancing quantum correlations in an optomechanical system via cross-Kerr nonlinearity, *J. Opt. Soc. Am. B* **34**, 1503 (2017).
 - [35] P. F.-Díaz, L. Lammata, E. Rico, and E. Solano, Ultrastrong

- coupling regimes of light-matter interaction, *Rev. Mod. Phys.* **91**, 025005 (2019).
- [36] A. F. Kockum, A. Miranowicz, S. D. Liberato, S. Savasta, and F. Nori, Ultrastrong coupling between light and matter, *Nature Reviews Physics* **1**, 19 (2019).
- [37] J. R. Carson, A generalization of reciprocal theorem, *Bell Sys. Tech. J.* **3**, 393 (1924).
- [38] R. Carminati, J. J. Sáenz, J.-J. Greffet, and M. N.-Vesperinas, Reciprocity, unitarity, and time-reversal symmetry of the S matrix of fields containing evanescent components, *Phys. Rev. A* **62**, 012712 (2000).
- [39] M. N.-Vesperinas, *Scattering and Diffraction in Physical Optics* (Word Scientific, Singapore, 2006).
- [40] A. A. Anappara, S. D. Liberato, Alessandro Tredicucci, Cristiano Ciuti, Giorgio Biasiol, Lucia Sorba, and Fabio Beltram, Signatures of the ultrastrong light-matter coupling regime, *Phys. Rev. B* **79**, 201303 (2009).
- [41] C. K. Law, Interaction between a moving mirror and radiation pressure: A Hamiltonian formulation, *Phys. Rev. A* **51**, 2537 (1995).
- [42] A. Schliesser, R. Rivière, G. Anetsberger, O. Arcizet, and T. J. Kippenberg, Resolved-sideband cooling of a micromechanical oscillator, *Nature Physics* **4**, 415 (2008).
- [43] K. Koshino, Semiclassical evaluation of the two-photon cross-Kerr effect, *Phys. Rev. A* **74**, 053818 (2006).
- [44] L. Mandel and E. Wolf, *Optical Coherence and Quantum Optics* (Cambridge University, UK, 1995).
- [45] T. T. Heikkilä, F. Massel, J. Tuorila, R. Khan, and M. A. Sillanpää, Enhancing Optomechanical Coupling via the Josephson Effect, *Phys. Rev. Lett.* **112**, 203603 (2014).
- [46] W. Xiong, D.-Y. Jin, Y. Qiu, C.-H. Lam, and J. Q. You, Cross-Kerr effect on an optomechanical system, *Phys. Rev. A* **93**, 023844 (2016).
- [47] Dustin Kleckner, William Marshall, Michiel J. A. de Dood, Khodadad Nima Dinyari, Bart-Jan Pors, William T. M. Irvine, and Dirk Bouwmeester, High Finesse Opto-Mechanical Cavity with a Movable Thirty-Micron-Size Mirror, *Phys. Rev. Lett.* **96**, 173901 (2006).
- [48] D. Vitali, S. Gigan, A. Ferreira, H. R. Böhm, P. Tombesi, A. Guerreiro, V. Vedral, A. Zeilinger, and M. Aspelmeyer, Optomechanical Entanglement between a Movable Mirror and a Cavity Field, *Phys. Rev. Lett.* **98**, 030405 (2007).
- [49] Y. Hu, G.-Q. Ge, S. Chen, X.-F. Yang, and Y.-L. Chen, Cross-Kerr-effect induced by coupled Josephson qubits in circuit quantum electrodynamics, *Phys. Rev. A* **84**, 012329 (2011).
- [50] E. T. Holland, B. Vlastakis, R. W. Heeres, M. J. Reagor, U. Vool, Z. Leghtas, L. Frunzio, G. Kirchmair, M. H. Devoret, M. Mirrahimi, and R. J. Schoelkopf, Single-Photon-Resolved Cross-Kerr Interaction for Autonomous Stabilization of Photon-Number States, *Phys. Rev. Lett.* **115**, 180501 (2015).
- [51] Y. Y. Gao, B. J. Lester, K. S. Chou, L. Frunzio, M. H. Devoret, L. Jiang, S. M. Girvin, and R. J. Schoelkopf, Entanglement of bosonic modes through an engineered exchange interaction, *Nature (London)* **556**, 509 (2019).
- [52] J. Majer, J. M. Chow, J. M. Gambetta, Jens Koch, B. R. Johnson, J. A. Schreier, L. Frunzio, D. I. Schuster, A. A. Houck, A. Wallraff, A. Blais, M. H. Devoret, S. M. Girvin, and R. J. Schoelkopf, Coupling superconducting qubits via a cavity bus, *Nature (London)* **449**, 443 (2007).
- [53] D. F. Walls and G. J. Milburn, *Quantum Optics* (Springer, Germany, 2008).
- [54] S. M. Barnett and P. M. Radmore, *Methods in Theoretical Quantum Optics* (Clarendon Press, Oxford, 1997).
- [55] S. Gröblacher, K. Hammerer, M. R. Vanner, and M. Aspelmeyer, Observation of strong coupling between a micromechanical resonator and an optical cavity field, *Nature (London)* **460**, 724 (2009).
- [56] J.-Q. Liao, J.-F. Huang, L. Tian, L.-M. Kuang, and C. P. Sun, Generalized ultrastrong optomechanical-like coupling, *Phys. Rev. A* **101**, 063802 (2020).
- [57] A. A. Clerk, M. H. Devoret, S. M. Girvin, F. Marquardt, and R. J. Schoelkopf, Introduction to quantum noise, measurement, and amplification, *Rev. Mod. Phys.* **82**, 1155 (2010).
- [58] M. O. Scully and M. S. Zubairy, *Quantum Optics* (Cambridge University, UK, 2011).
- [59] C. W. Gardiner and P. Zoller, *Quantum noise*, Germany (2000).
- [60] Daniel Manzano, A short introduction to the Lindblad master equation, *AIP Advances* **10**, 025106 (2020).
- [61] V. Gorini, A. Kossakowski, and E. C. Sudarsanan, Completely positive semigroups of n -level systems, *J. Math. Phys.* **17**, 821 (1976).
- [62] G. M. Moy, J. J. Hope, and C. M. Savage, Born and Markov approximations for atom lasers, *Phys. Rev. A* **59**, 667 (1999).
- [63] E. Knill, R. Laflamme, and G. J. Milburn, A scheme for efficient quantum computation with linear optics, *Nature (London)* **409**, 46 (2001).
- [64] S. Rips, M. Kiffner, W.-Rae, and M. J. Hartmann, Steady-state negative Wigner functions of nonlinear nanomechanical oscillators, *New J. Phys.* **14**, 023042 (2012).
- [65] Mohammad Hafezi and Peter Rabl, Optomechanically induced non-reciprocity in microring resonators, *Opt. Express* **20**, 7672-7684 (2012).
- [66] H. J. Kimble, Strong interactions of single atoms and photons in cavity QED, *Phys. Scr.* **1998**, 127 (1998).
- [67] J.-M. Pirkkalainen, S. U. Cho, Jian Li, G. S. Paraoanu, P. J. Hakonen, and M. A. Sillanpää, Hybrid circuit cavity quantum electrodynamics with a mechanical resonator, *Nature (London)* **494**, 211 (2013).
- [68] E. Verhagen, S. Deléglise, S. Weis, A. Schliesser, and T. J. Kippenberg, Quantum-coherent coupling of a mechanical oscillator to an optical cavity mode, *Nature* **482**, 63 (2012).
- [69] J. D. Teufel, T. Donner, D. Li, J. W. Harlow, M. S. Allman, K. Cicak, A. J. Sirois, J. D. Whittaker, K. W. Lehnert, R. W. Simmonds, Sideband cooling of micromechanical motion to the quantum ground state, *Nature (London)* **475**, 359 (2011).
- [70] J. C. Sankey, C. Yang, B. M. Zwickl, A. M. Jayich, and J. G. E. Harris, Strong and tunable nonlinear optomechanical coupling in a low-loss system, *Nat. Phys.* **6**, 707 (2010).
- [71] J.-Q. Liao and F. Nori, Single-photon quadratic optomechanics, *Scientific Reports* **4**, 6302 (2014).
- [72] E. M. Purcell, Spontaneous emission probabilities at radio frequencies, *Phys. Rev.* **69**, 681 (1946).
- [73] J. M. Raimond, Brune, M. Haroche, S. Manipulating quantum entanglement with atoms and photons in a cavity, *Rev. Mod. Phys.* **73**, 565 (2001).
- [74] T. Niemczyk, F. Deppe, H. Huebl, E. P. Menzel, F. Hocke, M. J. Schwarz, J. J. Garcia-Ripoll, D. Zueco, T. Hümmer, E. Solano, A. Marx, R. Gross, Circuit quantum electrodynamics in the ultrastrong-coupling regime, *Nature Physics* **6**, 772 (2010).
- [75] Andreas Bayer, Marcel Pozimski, Simon Schambeck, Dieter Schuh, Rupert Huber, Dominique Bougeard, and Christoph Lange, Terahertz light-matter interaction beyond unity coupling strength, *Nano Lett.* **17**, 6340 (2017).
- [76] Anton Frisk Kockum, Adam Miranowicz, Simone De Liberato, Salvatore Savasta, and Franco Nori, Ultrastrong coupling between light and matter, *Nature Reviews Physics* **1**, 19-40 (2019).
- [77] E. X. DeJesus and C. Kaufman, Routh-Hurwitz criterion in the

- examination of eigenvalues of a system of nonlinear ordinary differential equations, *Phys. Rev. A* **35**, 5288 (1987).
- [78] C. W. Gardiner and M. J. Collett, Input and output in damped quantum systems: Quantum stochastic differential equations and master equation, *Phys. Rev. A* **31**, 3761 (1985).
- [79] G. S. Agarwal, and S. Huang, Optomechanical systems as single-photon routers, *Phys. Rev. A* **85**, 021801 (R) (2012).
- [80] Darrick E. Chang, Anders S. Sørensen, Eugene A. Demler, and Mikhail D. Lukin, A single-photon transistor using nanoscale surface plasmons, *Nature Physics* **3**, pages 807–812 (2007).
- [81] X. W. Xu and Y. Li, Optical nonreciprocity and optomechanical circulator in three-mode optomechanical systems, *Phys. Rev. A* **91**, 053854 (2015).
- [82] H. Mäkelä and M. Möttönen, Effects of the rotating-wave and secular approximations on non-Markovianity, *Phys. Rev. A* **88**, 052111 (2013).
- [83] Daniel Malz and Andreas Nunnenkamp, Optomechanical dual-beam backaction-evading measurement beyond the rotating-wave approximation, *Phys. Rev. A* **94**, 053820 (2016).
- [84] L. Novotny and B. Hecht, *Principles of Nano-Optics* (Cambridge University, UK, 2012).
- [85] Cheng Shang, H. Z. Shen, and X. X. Yi, Nonreciprocity in a strong coupled three-mode optomechanical circulatory system, *Optics Express* **27**, 18 (2019).
- [86] Mohammad-Ali Miri, Freek Ruesink, Ewold Verhagen, and Andrea Alù, Optical Nonreciprocity Based on Optomechanical Coupling, *Phys. Rev. Applied* **7**, 064014 (2017).
- [87] Yi-Bing Qian, Deng-Gao Lai, Mei-Ran Chen, and Bang-Pin Hou, Nonreciprocal photon transmission with quantum noise reduction via cross-Kerr nonlinearity, *Phys. Rev. A* **104**, 033705 (2021).
- [88] Z. L. Xiang, S. Ashhab, J. Q. You, and F. Nori, Hybrid quantum circuits: Superconducting circuits interacting with other quantum systems, *Rev. Mod. Phys.* **85**, 623 (2013).
- [89] J. Q. You and F. Nori, Atomic physics and quantum optics using superconducting circuits, *Nature (London)* **474**, 589 (2011).
- [90] J. M. Pirkkalainen, S. U. Cho, F. Massel, J. Tuorila, T. T. Heikkilä, P. J. Hakonen, Cavity optomechanics mediated by a quantum two-level system, *Nat. Commun.* **6**, 6981 (2015).
- [91] M. A. Sillanpää, Leif Roschier, and P. J. Hakonen, Inductive single-electron transistor (L-SET). *Phys. Rev. Lett.* **93**, 066805 (2004).
- [92] G. S. Agrwal and S. Huang, Electromagnetically induced transparency in mechanical effects of light, *Phys. Rev. A* **81**, 041803(R) (2010).
- [93] S. Weis, R. Rivière, S. Deléglise, E. Gavartin, O. Arcizet, A. Schliesser, and T. J. Kippenberg, Optomechanically induced transparency, *Science* **330**, 1520 (2010).
- [94] A. H. Safavi-Naeini, T. P. M. Alegre, J. Chan, M. Eichenfield, W. Winger, Q. Lin, J. T. Hill, D. E. Chang, and O. Painter, Electromagnetically induced transparency and slow light with optomechanics, *Nature (London)* **472**, 69 (2011).
- [95] D. Vitali, S. Gigan, A. Ferreira, H. R. Böhm, P. Tombesi, A. Guerreiro, V. Vedral, A. Zeilinger, and M. Aspelmeyer, Optomechanical Entanglement between a Movable Mirror and a Cavity Field, *Phys. Rev. Lett.* **98**, 030405 (2007).
- [96] Y.-F. Jiao, S.-D. Zhang, Y.-L. Zhang, A. Miranowicz, L.-M. Kuang, and H. Jing, Nonreciprocal Optomechanical Entanglement against Backscattering Losses, *Phys. Rev. Lett.* **125**, 143605 (2020).
- [97] S. Barzanjeh, A. Xuereb, S. Gröblacher, M. Paternostro, C. A. Regalet, and Eva M. Weig, Optomechanics for quantum technologies, *Nature Physics*, **18**, 15-24 (2022).
- [98] M.-A. Miri, Freek Ruesink, Ewold Verhagen, and Andrea Alù, Optical nonreciprocity based on optomechanical coupling, *Phys. Rev. Applied* **7**, 064014 (2017).
- [99] F. Ruesink, M.-A. Miri, Andrea Alù, Ewold Verhagen, Nonreciprocity and magnetic-free isolation based on optomechanical interactions, *Nature communications* **7**, 1-8 (2016).